



RESEARCH & DEVELOPMENT

Intelligent Data Exploration & Analysis for New & Existing Transportation Technology (IDEANETT)

John Park, PhD, Associate Professor

**Department of Engineering Management & Systems Engineering
Old Dominion University**

Venktesh Pandey, PhD Assistant Professor,

**Department of Civil, Architectural and Environmental Engineering
North Carolina A& T State University**

NCDOT Project TCE2020-01

FHWA/NC/2020-60

AUGUST 2023

TECHNICAL REPORT DOCUMENTATION PAGE

1. Report No. FHWA/NC/2020-60	2. Government Accession No.	3. Recipient's Catalog No.	
4. Title and Subtitle Intelligent Data Exploration & Analysis for New & Existing Transportation Technology (IDEANETT)		5. Report Date July 31 2023	
		6. Performing Organization Code	
7. Author(s) John Park, PhD; Venkatesh Pandey, PhD; Larkin Folsom (PhD); Justice Darko (PhD); Niharika Deshpande.		8. Performing Organization Report No.	
9. Performing Organization Name and Address Old Dominion University, 2101F Engineering Systems Building, Norfolk, VA 23529 North Carolina A& T State University, 1601 E. Market St, McNair Hall 434, Greensboro, NC 27411		10. Work Unit No.	
		11. Contract or Grant No. FHWA/NC/2020-60	
12. Sponsoring Agency Name and Address North Carolina Department of Transportation Research and Development Unit 1020 Birch Ridge Drive Raleigh, NC 27610		13. Type of Report and Period Covered Final Report (February 2020 to July 2023)	
		14. Sponsoring Agency Code	
15. Supplementary Notes Conducted in cooperation with the U.S. Department of Transportation, Federal Highway Administration.			
16. Abstract Unforeseen elements such as road closures, accidents, and adverse weather conditions significantly impact the traffic delays during daily commutes. Effective alleviation of these delays can be achieved through careful rerouting of travelers, guided by real-time traffic information. This project focuses on reducing traffic congestion by examining the interplay between two distinct groups of drivers – those with access to rerouting information and those without – through the lens of simulation modeling and traffic equilibrium. Under a mixed information framework, a navigation app provides within-day route suggestions to informed drivers using predicted information about the time-varying route habits of uninformed drivers. The informed users detour from initially proposed routes to minimize network congestion after traffic disruptions, pushing the system toward optimal equilibrium, while uninformed drivers make day-to-day decisions which push the system toward user equilibrium. Simulations considering varying fractions of informed drivers show that congestion is reduced during abrupt phase transition before reaching equilibrium by approximately 59.2% when 20% of drivers are informed and is nearly eliminated when 80% of drivers are informed, which could be achieved through connected vehicle technologies. Furthermore, this research explores a new family of decision-making models that can indirectly learn and transfer online information from simultaneous observations of a probability distribution. Analysis on 39 link segments on I540 near Raleigh, NC demonstrate that the proposed method is useful in getting more accurate travel time predictions ahead of time. Broadly, the proposed methods contribute towards data-intelligent techniques for evaluation and planning of transportation systems under uncertainty.			
17. Key Words Informed routing, predictive informatics, bounded rationality, mixed information, congestion phase			18. Distribution Statement
19. Security Classif. (of this report) Unclassified	20. Security Classif. (of this page) Unclassified	21. No. of Pages 53	22. Price

DISCLAIMER

The contents of this report reflect the views of the author(s) and not necessarily the views of the University. The author(s) are responsible for the facts and the accuracy of the data presented herein. The contents do not necessarily reflect the official views or policies of either the North Carolina Department of Transportation or the Federal Highway Administration at the time of publication. This report does not constitute a standard, specification, or regulation.

Acknowledgements

Three PhD students worked on this project to be part of their thesis: Larkin Folsom (PhD), Justice Darko (PhD), Niharika Deshpande.

Table of Contents

Acknowledgements	iii
Table of Contents	iv
List of Figures	v
List of Tables	vi
Executive Summary	1
Introduction	1
Dynamic Routing of Heterogeneous Users	1
Temporal Multimodal Machine Learning	3
Literature Review	5
Part 1: Dynamic Routing of Heterogeneous Users	7
Methodology	7
Novel Mixed Objective Framework	7
Dynamic Network Loading Model	9
Uninformed Driver Model	14
Results	23
Experimental Design and Procedure	23
Scenario Design	24
Conclusion	31
The Limitation and Future Study	32
Part 2: Temporal Multimodal Machine Learning	34
Methodology	34
Multimodal Learning	35
The Limitation and Future Study	40
References	41

List of Figures

Figure 1 Concept DTA flow diagram	2
Figure 2 Temporal Multimodal Learning (TML) from correlation of time-varying bimodal distributions between links.	4
Figure 3 Sioux Falls Network average Effective Path Delay for path 2,400, out of 6,180 paths, for each day and departure time window for uninformed drivers under bounded rationality. src = d1.....	8
Figure 4 Mixed Objective Model combining DTD BRDUE and WD DSO driver groups.	9
Figure 5 Example link occupancy curve	11
Figure 6 Triangular fundamental diagram.....	12
Figure 7 junction dynamic example	14
Figure 8 Sioux Falls Network perceived cost in seconds for path 2,400 , out of 6,180 paths, for each day and departure time window	15
Figure 9 Effect of varying the number of threads and the fraction of parallelizable code on speedup	22
Figure 10 Example of the available routes between nodes 1 and 4 in the Sioux Falls Network.	23
Figure 11 Sioux Falls Network average travel time for uninformed drivers seeking BRDUE.....	25
Figure 12 (A) Initial network departures on Day 1 based on initialized O-D demand, prior to informed drivers switching routes. (B) Initial delays on Day 1 based on initialized O-D demand, prior to informed drivers switching routes. (C) Network departures on Day 1 with DSO seeking route choices by the informed driver group. (D) Network delays on Day 1 with DSO seeking route choices by the informed driver group. (E): Uninformed DUE Avg. Excess TT on Day 1. (F) Mixed Objective Avg. Excess TT on Day 1.....	27
Figure 13 (A) Initial network departures on Day 2 based on initialized O-D demand, prior to informed drivers switching routes. (B) Initial delays on Day 2 based on initialized O-D demand, prior to informed drivers switching routes. (C) Network departures on Day 2 with DSO seeking route choices by the informed driver group. (D) Network delays on Day 2 with DSO seeking route choices by the informed driver group. (E) Uninformed DUE Avg. Excess TT on Day 2. (F) Mixed Objective Avg. Excess TT on Day 2.....	28
Figure 14 Day 1 and Day 2 O-D Gap for all paths with 0% informed drivers, 20% informed drivers, 40% informed drivers, and 80% informed drivers.	29
Figure 15 Left: Day 1 O-D gap for all paths under varying fractions of informed drivers. Right: Day 2 O-D gap for all paths under varying fractions of informed	31
Figure 16 Average Travel Time under varying fractions of informed.....	31
Figure 17 Online gain in temporal, multimodal, and multivariate prediction uncertainty between prior and posterior. Each cell can be assumed to have a combination of discrete travel time distributions (i.e., 2, 5, 10, 30min) with different weights.	34
Figure 18 Two steps in KF-TML: In the predict step, a model is employed to predict the chosen state variable at next time interval $t+1$ using measurement from previous time interval (k). In the update step, the predicted state is corrected using the noisy measurements at $t+1$	37
Figure 19 Speed predictions with and without TML and corresponding observations	39
Figure 20 Percent change in uncertainty of KF prediction when TML is considered.	40

List of Tables

Table 1 Table of Notation.....	9
--------------------------------	---

Executive Summary

This project focuses on reducing traffic congestion using the competing strategies between informed and uninformed drivers. Under a mixed information framework, a navigation app provides within-day route suggestions to informed drivers using predicted information about the time-varying route habits of uninformed drivers. The informed users detour from initially proposed routes to minimize network congestion after traffic disruptions, pushing the system toward optimal equilibrium, while uninformed drivers make day-to-day decisions which push the system toward user equilibrium. Simulations considering varying fractions of informed drivers show that congestion is reduced during abrupt phase transition before reaching equilibrium by approximately 59.2% when 20% of drivers are informed and is nearly eliminated when 80% of drivers are informed, which could be achieved through connected vehicle technologies. Shared memory multi-core parallelization improved computational efficiency. The second part of this project introduces temporal multimodal multivariate learning, a new family of decision-making models that can indirectly learn and transfer online information from simultaneous observations of a probability distribution with more than one peak or more than one outcome variable from one time stage to another. These findings provide a data-driven approach for evaluating the impact of information in travelers' choices. As agencies like NCDOT continue to deploy sensors and dynamic message signs, we recommend doing a careful modeling of changes in travelers' routes using the techniques presented in this research.

Introduction

Daily commutes can be unexpectedly protracted by road closures, accidents, and inclement weather. The quick restoration of traffic flow through the coordinated responses of emergency vehicles may help alleviate the traffic delays impacting the road network. However, the delays, which can exceed users' planned commuting time, can cause missed meetings, canceled appointments, and child care fees, accumulating costs. The majority of users react similarly to the unforeseen traffic delays and may unknowingly, collectively transfer congestion from one route to another. Current navigation systems (e.g., Google Maps) are not customized to users' tolerance for unexpected delays therefore they cannot predict optimal routes. Because the network is dynamic, the route suggestion users receive at the outset of their commute may not be optimal when they are on the road. In the literature, other traffic sensing technologies commonly fail to provide network-scale predictions under unexpected conditions. For example, current dynamic route choice models consider that the link travel time realization is only based on nearby links. The multimodal multivariate uncertainty caused by unobserved varying traffic patterns through the day has not been considered. Motivated by these challenges, this project focuses on developing two new approaches: 1) dynamic routing of heterogeneous users after traffic disruptions under a mixed information framework and 2) temporal multimodal Machine Learning to improve travel time prediction accuracy.

Dynamic Routing of Heterogeneous Users

Dynamic Traffic Assignment (DTA) algorithms have been used to capture dynamic interaction between supply and demand under equilibrium and non-equilibrium conditions in a transportation network. The two optimal conditions for a transportation network are Dynamic User Equilibrium (DUE) and Dynamic System Optimal (DSO) equilibrium (Yu et al., 2020). Most DTA algorithms solve for one of Wardrop's equilibrium conditions using a single group of drivers who share a common objective of minimizing their own travel cost or the total system cost. This research considers a novel application of DTA which realistically simulates a transportation network in which drivers have different objectives and different time scales over which they make decisions in an attempt to optimize the system. We define informed drivers as the ones who are given predictive route guidance from a system manager (e.g., traffic operation center) through GPS-based applications and assume that these drivers will make a bounded route choice with the provided guidance. Informed drivers are expected to comply with the provided guidance if they are given sufficient incentives and/or if the new route is not noticeably different from the original choice in terms of the cost. Such compliance will become more practical with shared autonomous vehicles that are expected to lower traveler's disutility of travel time through credits from the company for following those suggestions.

The role of information is especially relevant under expected and unexpected disruptions to infrastructure. Transportation networks are commonly impacted by short-term and long-term disruptions caused by natural or man-made events. For example, a multi-day construction zone on a highway can increase the travel time if travelers continue to follow the same route. Similarly, a post disaster event such as flooding of neighborhood streets or a tree collapse may

result in reduced capacity on certain links. In this study, we propose a mixed objective framework (Figure 1) that provides a method for a group of informed drivers to reduce the within-day congestion caused by uninformed drivers who are making choices based on day-to-day habits on route and departure time after a traffic disruption. Informed drivers are provided with the within-day route guidance based on the anticipated behaviors of uninformed drivers on the network day-to-day, by adjusting route choices toward system optimum. We assume that day-to-day evolution follows the same framework as the iterative process of DTA models and accurately simulates the iterative day-to-day transition of the adaptive and bounded behavior of uninformed drivers during the disruption of a transportation network. The resulting congestion patterns are caused by uninformed drivers' discrete decision-making processes before reaching equilibrium. The day-to-day decision-making of uninformed drivers may result in congestion depending on levels of perturbations and network congestion. This research presents a methodology to reduce the congestion caused by uninformed users making day-to-day decisions by strategically rerouting informed drivers. The within-day traffic dynamics are incorporated into the simulation at the end of the day to reoptimize (offline) next day's informed driver strategy considering day-to-day dynamics of uninformed drivers. For an application to a post disaster event, day 1 of the model is after loading within-day travel behaviors of the day of the collapse. The methodology applied to inform human drivers in this research is also applicable to Connected Autonomous Vehicles (CAVs) operating in mixed autonomy networks.

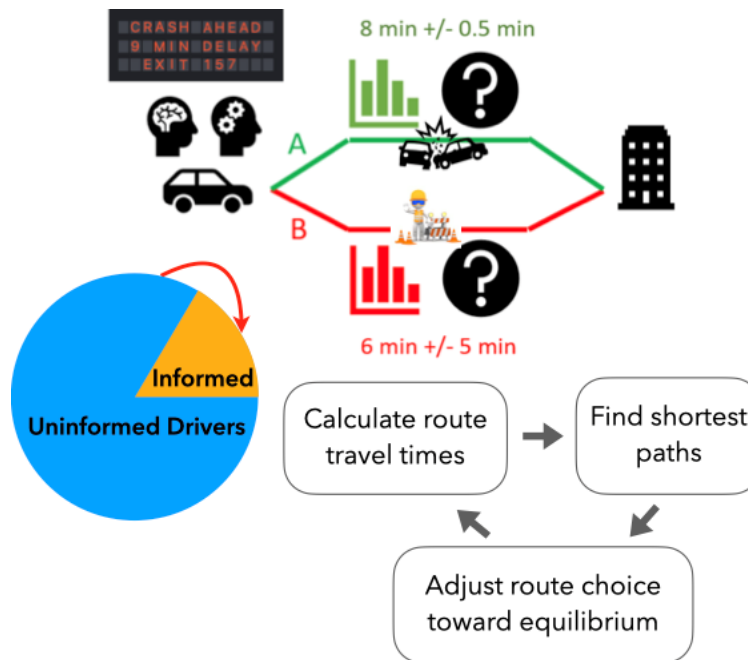


Figure 1 Concept DTA flow diagram

Modern DTA algorithms use a Dynamic Network Loading (DNL) procedure to simulate traffic dynamics on a transportation network (Osorio et al., 2011). The procedure incorporates a cell or link transmission model and considers junction dynamics. In the presented model, the DNL procedure is used for two separate groups of drivers who are seeking different objectives over

different time scales. Uninformed drivers make route choices to seek Day-to-Day (DTD) Boundedly Rational (BR) DUE. Informed drivers take detours to seek Within-Day (WD) DSO equilibrium within their indifference band, not blindly following the recommendation from a phone app or system manager. This assumption is justified because the routes for informed travelers can be selected by the system manager such that system efficiency improves, while the uninformed travelers choose routes selfishly to minimize their own time. The approach taken in this research is an upper-level algorithm that solves for Day-to-Day BRDUE and a lower-level algorithm that solves for WD DSO equilibrium. Each DTD BRDUE iteration considers the prior day's route and departure time choices and uses this information to solve for the next day. A DTD BRDUE algorithm will not achieve equilibrium on day one, because each user must complete their trip on a given Origin-Destination (O-D) pair to make an informed decision on their next trip, which occurs the following day. This method more accurately simulates the way that a transportation network approaches BRDUE following a perturbation to the network dynamics, such as construction or a change in signal timings.

When the network is perturbed, users will experience significant delays on the day of the perturbation because the route and departure time choices for uninformed drivers are based on their experience with the prior day's trip and their memory of other trips. If a serious delay occurs, their route and departure time choice the next day will consider this new information. In order to improve this framework by addressing Within-Day delays, a WD DSO algorithm that reacts to predictable delays caused by the behavior of DTD BRDUE seeking users is proposed. The WD DSO algorithm influences the decision-making of a subset of the population of drivers by providing them with predictive information in order to push the system toward DSO equilibrium.

Temporal Multimodal Machine Learning

Recent Google Deep-mind research has been using many factors and real-time updates of traffic data for more accurate prediction of travel time. Anticipatory routing guidance is effective in knowledge transfer, however, ignores the potential information gain from probability density functions with more than one peak. Consider a network with a grid laid on top in Figure 1, where each cell represents a small geographical region. To find an optimal route from an origin cell to a destination, forecasting the condition of intermediate cells is critical. Routing literature did not use a location's observed data to forecast conditions at distant non-contiguous locations' unobserved data. We aggregate the data from all cells in the grid and cluster cells that have similar combinations of probability distributions. When one cell of a cluster is explored, the information gained from the explored cell can partially remove uncertainty about the conditions in distant non-contiguous unexplored cells of the same cluster.

Here's another example demonstrating the multimodal traffic learning: assume we know a freeway link \mathbb{A} historically takes 2-minutes without congestion but it may take 8 minutes due to an unexpected event (e.g., incidents). We can cluster \mathbb{A} and \mathbb{A}' in the same correlated group assuming the bimodal travel distributions for both links are similar. Literature ignores three benefits of sending a platoon of vehicles to \mathbb{A} instead of \mathbb{B} shown at the bottom in Figure 3: For a scenario that turned out to be 2 minutes due to the fast clearance of the incident, 1) we can update the predicted travel time on this link \mathbb{A} so other drivers can switch either their departure time or route to take this 2-minutes shortcut, 2) we can update travel time on other links (e.g., \mathbb{A}'

) having the same type of probability distributions. By knowing that the total travel time of a route is 4-minutes, we can send more vehicles to this route and relieve other route congestion that turned out to be 8-minutes due to the long clearance of the incident, 3) we update travel time on other links (e.g., A') having the same type of probability distributions. By knowing that the total travel time of a route A' is 16-minutes, we can inform fewer vehicles to use this route, redistribute traffic to other routes (i.e., BC) having shorter travel times. While the current routing literature realize only nearby links, the realization of multimodal travel time distributions that are derived from real-world data have not been studied. However, recent studies have shown that travel time distributions on freeways have two or more modes as distinct peaks in the probability density function due to the mixes of driving patterns and vehicle types. This multimodal (or bimodal) distribution exists on arterial roads, where a vehicle passing a signal at the end of the green would experience quite different travel time than the vehicle following behind it that must make a stop at the red, although they traveled next to each other. Without knowing the future traffic with confidence, the traditional choice theory considers the bounded rationality of the majority of agents taking a detour to link B , which causes congestion on B and nearby roads (In Figure 2).

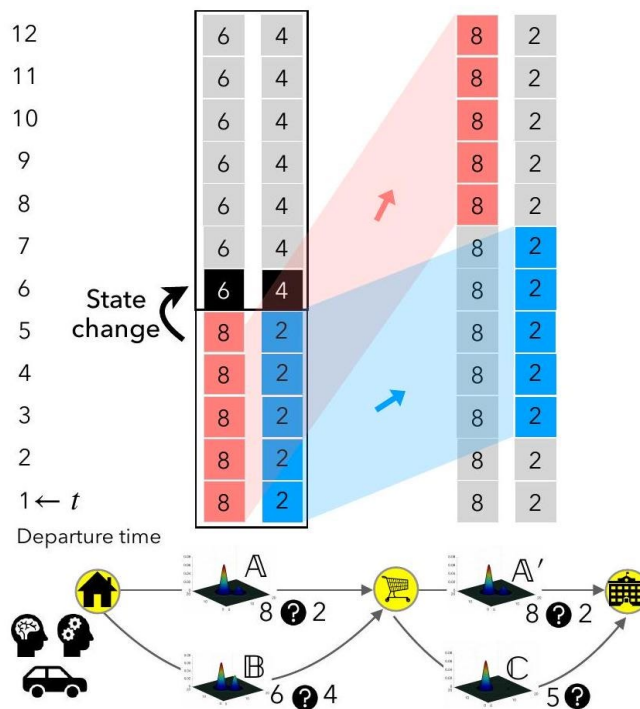


Figure 2 Temporal Multimodal Learning (TML) from correlation of time-varying bimodal distributions between links.

A has a bimodal distribution with a mode at 8 and 2 between time stages 1 to 5, switching to a bimodal distribution with a mode at 6 and 4 at time stage 6. For departing at time stage 1, the time-invariant method adds travel time together either the high or low modes of link and route AA' travel time to be either $8 + 8$ or $2 + 2$. The timevariant method accounts for the time needed to traverse A either 8 or 2 minutes and re-evaluates the travel time at A' based on the time of entering A' , may encourage a detour to Link C in case of 8 minutes of realization. We assume that the state change is given based on event models.

The previous examples assume that the primary factor contributing to travel time variation on a given link is the time of day. The focus of this study is to use travel time correlation information to remove uncertainty in within-day travel. Travel time may depend on other factors such as day-of-week, weather patterns during the day, and special events in the region like post-game-day traffic near a sports stadium. If data on these other variables are made available, the same temporal learning process can be extended.

Literature Review

Mathematical methods of achieving time-dependent User Equilibrium (UE) and System Optimal (SO) equilibrium conditions in transportation networks were established by Peeta and Mahmassani (1995). The authors found that when congestion becomes very high, the ability to reroute vehicles decreases due to gridlock. Under these conditions, rerouting vehicles fail to substantially reduce congestion. Recently, information sharing between Day-to-Day (DTD) Boundedly Rational Dynamic User Equilibrium (BRDUE) seeking agents in a DTA simulation has been explored (Han et al., 2019; Yu et al., 2020). Within-Day (WD) Dynamic System Optimal (DSO) DTA problems have also been solved using a novel projection model in conjunction with a cell transmission model (Doan and Ukkusuri, 2015). A mixed behavior model of UE and stochastic UE in DTD route flow evolution was modeled (Zhou et al., 2017). In line with those advances, in this paper, we provide the drivers with predicted information of the future state during the critical period when they can change the decision before reaching equilibrium, especially when we still have room to reroute a subset of vehicles that can reduce congestion. Below, we review proactive routing guidance under uncertain information to reach BRDUE and BRDSO considering time-varying route habits of drivers.

A proactive route guidance was proposed to assign users to a small subset of all the possible paths considering the maximum travel inconvenience allowed (Angelelli et al., 2018), then the solution was extended to column generation algorithm to improve the exponentially increasing size of the path (Angelelli et al., 2021). The Predictive DUE (PDUE) condition in which a user chooses a route that minimizes the actual travel time along the route to the user's destination while anticipating the future traffic state has been explored (Varia et al., 2013). The PDUE concept has been successfully applied to macroscopic pedestrian flow models (Jiang et al., 2016). The possibility to solve for a PDUE condition in congested capacity-constrained networks using DTA and the method of successive averages (MSA) has been demonstrated (Yildirimoglu and Geroliminis, 2014; Yildirimoglu et al., 2015; Yu et al., 2020). DTA using mesoscopic fundamental diagram dynamics has been applied to a multi-region network composed of 3 regions and 19 sub-regions (Yildirimoglu et al., 2015). Results showed that using route guidance to push a network toward a system optimal condition does not penalize a significant proportion of drivers. The route choice behavior with information under uncertainty was investigated (Avineri and Prashker, 2006). Analysis of the effects on transportation networks by human drivers operating under mixed information on simple single Origin-Destination (O-D) networks with two route choices was performed (Litescu et al., 2015; Litescu et al., 2016b). Prior research examining the effects of informed and uninformed drivers indicated that the stability of the network is dependent upon the percentage of informed drivers (Litescu et al., 2015). In a network in which drivers are given a choice over the route, but not departure time, the authors

demonstrated that a level of approximately 40% informed drivers provides optimal network performance; however, network instability arises when the number of informed drivers deviates from the optimal percentage (Litescu et al., 2015). The authors did not investigate predictive decision making by informed drivers, rather the authors assumed that informed drivers make instantaneous decisions based on the current state of the network.

Additional evaluation of the effects of information uncertainty under the same network and conditions was performed (Litescu et al., 2015; Litescu et al., 2016b). The authors determined when informed drivers receive imperfect information, the equilibrium condition for a transportation network is still highly correlated with the fraction of informed drivers, with the level of 40% informed drivers being the most robust to information inaccuracy under the conditions of the study. Agent-based behavioral models of driver compliance with Variable Message Sign (VMS) suggestions based on survey data have been developed (Litescu et al., 2015). The author considered the effects of VMS on drivers in a simulation of the Brisbane Western corridor. Several model application areas were identified, including varying the type and accuracy of the presented information, as well as varying the fraction of users provided with information. Research has demonstrated that dynamic perturbations to traffic light timing can negatively impact congestion under light traffic loads, due to drivers' difficulty in predicting the behavior of the traffic light (Litescu et al., 2016a). DTA literature has focused on estimating the impact of information on bounded choice and mitigating traffic congestion under DUE and DSO conditions, either within-day or day-to-day.

Mahmassani and his colleagues have shown that the “indifference band” of commuters may cause them not to switch to shorter paths even all path cost information is available to travelers (Mahmassani and Jayakrishnan, 1991; Mahmassani and Liu, 1999; Mahmassani, 2001). Boundedly rational dynamic user equilibrium (BRDUE) and variable tolerance boundedly rational dynamic user equilibrium (VT- BRDUE) problems have been analyzed (Simon, 1962; Han et al., 2015). In the latter problem, the path used and actual departure rates determine the tolerances of boundedly rational users in system. A comprehensive review of models and methodologies for boundedly rational route choice behavior was composed by Di and Liu (2016). The authors note that models which assume perfect rationality suffer from estimation and prediction errors. Additionally, human behavior under stable situations is myopic as well as significantly based upon formed habits (Jotisankasa and Polak, 2006; Di and Liu, 2016). Unified methods for determining driver route choice behavior with models that consider bounded rationality and learning mechanisms have been considered (Di and Liu, 2016). The use of thresholds has been considered for updating driver perceptions when a discrepancy between perceived travel time and experienced travel time exists (Jotisankasa and Polak, 2006). The consequences of BRUE on the Braess paradox, which describes the paradoxical discovery that the addition of more links to a transportation network can worsen travel times, have been explored (Di et al., 2014). The Braess paradox is largely addressed by bounded rationality, but can still occur for travel demands which fall within a certain range. The authors found that the Braess paradox can be avoided by reducing discrepancies between selfish routing and optimal routing.

Real-world agents have been shown to repeat habitual behavior until prompted to search for alternatives, for example, when searching for different mechanisms of meeting their travel demand (Xiong et al., 2015) with data-driven methods (Zhu et al., 2010). Bias caused by self-

reporting preference data and driving simulators' impact of en-route diversion decisions under real-time information has been considered (Xiong and Zhang, 2013a). Modeling of agent level departure time choice under uncertainty has demonstrated that under high uncertainty, agents do not easily converge on an optimized equilibrium (Xiong and Zhang, 2013b). Research has demonstrated that flexible work schedules allow departure times to vary more greatly which reduces congestion in a transportation network (Zhu et al., 2015). The authors found that congestion could be reduced even when a relatively small percentage (10–20%) of road users had flexible work schedules. Agent-based simulations of an interstate corridor in Washington, D.C. have revealed that 6.2% of trips during peak-hours will switch departure times to avoid congestion (Zhang et al., 2013).

Part 1: Dynamic Routing of Heterogeneous Users

To summarize, there are four contributions of this project regarding congestion mitigation:

- This project extends the mixed information framework by providing within-day route suggestions to informed drivers using predicted information about the time-varying route habits of uninformed drivers. The informed users detour from initially proposed routes to minimize network congestion after traffic disruptions, pushing the system toward optimal equilibrium, while uninformed drivers make day-to-day decisions which push the system toward user equilibrium.
- This project predicts the delay caused by random perturbation through DTD BRDUE simulation and provides WD DSO decision-making for informed drivers, while considering their bounded rationality. Rather than computationally intensive MSA, we only suggest a small subset of feasible alternative paths within small changes of original utility.
- This project introduces a new predictive and mixed information framework of competing strategies between informed and uninformed drivers and further reduces traffic congestion.
- This project captures the effect of perturbation by approximating path marginal cost (PMC) for each path and solve BRDSO DTA while avoiding overestimation (Peeta and Mahmassani, 1995) and underestimation of PMC (Qian and Zhang, 2011; Qian et al., 2012).

Methodology

Novel Mixed Objective Framework

Unlike prior research, the presented model contains a mixture of informed and uninformed drivers with different routing behaviors towards reaching equilibrium across different time scales. Uninformed drivers make their route and departure time choices based on the memory of their own prior effective travel cost (Han, Eve, and Friesz, 2019) and selfishly seek to minimize their own travel time (Wardrop, 1952). If all drivers are uninformed, the route choices will iteratively converge to the BRDUE conditions. The informed drivers in the presented model are assumed to be accessing an app, which they use to determine their route and departure time choice. The informed drivers make within-day decisions based on the information presented by the app, which suggests the best routes based on the predicted network state for that day. Unlike the uninformed drivers, informed drivers are given routes that seek to push the

system toward WD DSO equilibrium. Informed drivers' route and departure time choices are calculated using a separate within-day DNL procedure. The within-day DNL procedure is used to calculate the PMC for each route and departure time. PMC considers the additional delay on all other drivers when an informed driver chooses a given route and departure time.

- Group 1 (Uninformed): Choose route and departure time based on Effective Path Delay simulated in Figure 2), using DTD BRDUE DTA algorithm, influenced the transition between the presence of perturbations and after removal of perturbations. Details on the network is in the scenario design of result section. These drivers are selfishly seeking to minimize their own travel time (Wardrop, 1952).
- Group 2 (Informed): Choose route and departure time using a smart phone navigation app, which suggests routes with the least PMC. This is calculated using a within-day DTA algorithm. These drivers are directed to push the system toward DSO, mitigating congestion caused by the inability of uninformed drivers to predict perturbations in the network.

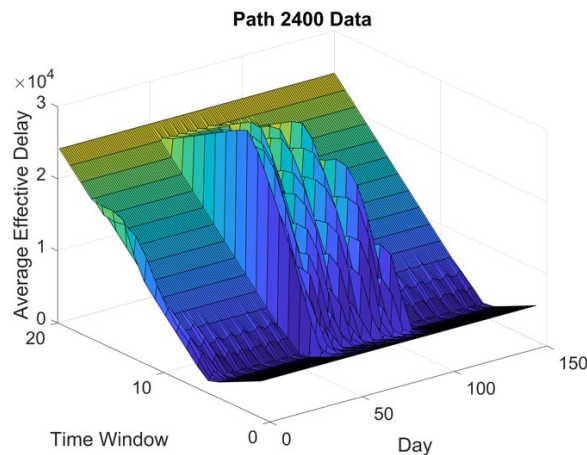


Figure 3 Sioux Falls Network average Effective Path Delay for path 2,400, out of 6,180 paths, for each day and departure time window for uninformed drivers under bounded rationality. src = d1

The extent to which Group 2 (Informed drivers) can be rerouted is subject to additional constraints based on information gained for other informed drivers and their own indifference bands. Informed drivers need to be convinced to choose a system optimal route and it will only work over time if the maximum deviation from a user optimal route is within their indifference band, which is defined as a range of total travel times over which the informed travelers are indifferent. For example, if the shortest travel time at DUE between an OD pair is Z units and the indifference band for an informed traveler is z units, then informed travelers are convinced to switch their routes and departure times based on their experienced travel time such that their resulting travel time is at most $Z + z$. In our simulations, we assume the range of indifference band is up to 400 s following Han et al. (2019). This system more closely approximates the mixed autonomy and mixed information conditions that are likely to be encountered in transportation networks during the next decade. This research is particularly applicable to smaller and mid sized cities where less information is available and uninformed drivers are more likely to repeatedly use the same route based only on past experience. The total system costs

are then compared across the two scenarios: (a) the DTD BRDUE algorithm alone and (b) the mixed information diagram in Figure 4 outlines the general framework. The mixed objective model starts from the initialization of the demand for each O-D pair at each departure time without informed drivers switching routes, run day to day and within-day DNL until the minimum solution is found in DSO with informed drivers strategy for a fixed number of days.

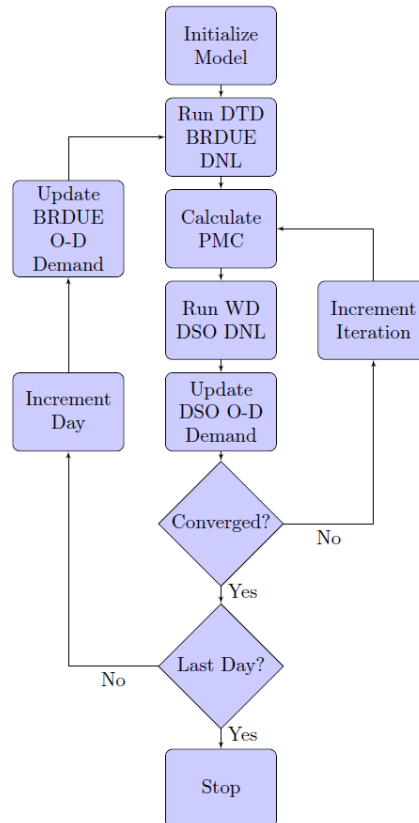


Figure 4 Mixed Objective Model combining DTD BRDUE and WD DSO driver groups.

Dynamic Network Loading Model

Han et al. (2019) described the BRDUE DNL framework presented in this section in their research. Table of notations (Table 1) summarizes all the notations used in this paper.

Table 1 Table of Notation.

N	\triangleq	Set of all nodes n
\mathcal{L}	\triangleq	Set of all directed links
\mathcal{P}	\triangleq	Set of all OD pairs $[r, s]$
K	\triangleq	Set of all routes across the network

T	\triangleq	Set of all discrete time intervals
For OD pair $[r, s] \in \mathcal{P}$		
K_{rs}	\triangleq	Set of all routes connecting $[r, s]$
d_{rs}	\triangleq	OD demand $[r, s]$
$\mathcal{R}_{rs}(t)$	\triangleq	Set of all canonical routes connecting $[r, s]$ for departure time t
TA_{rs}	\triangleq	Desired arrival time at the destination for all travelers traveling across $[r, s]$
For a route $k \in K$ and departure time $t \in T$		
$h_k(t)$	\triangleq	Total path flow departing on route k at time t
$\Pi_k(t)$	\triangleq	Travel time on route k for time t
$SDC_k(t)$	\triangleq	Schedule delay cost on route k for time t
$PC_k(t)$	\triangleq	Total cost
$PMC_{k,t}$	\triangleq	Path Marginal cost
Parameters		
Θ	\triangleq	Relative range around shortest travel time for defining canonical routes
θ and θ_2	\triangleq	Scaling parameters for Mlogit model
Δ and Δ_2	\triangleq	Bounded-rationality indifference band
κ_{informed}	\triangleq	Proportion of travelers who are informed

Consider a traffic network represented by a directed graph $G = (\mathcal{N}, \mathcal{L})$ consisting of set \mathcal{N} of all nodes, and set \mathcal{L} of all directed links. The network is dynamic where set T denote the set of all discrete time interval indices ranging from $1, 2, \dots, |T|$, where each interval is one time unit wide; for our experiments, we consider each time unit to be 6 s.

Let $\mathcal{P} \subseteq \mathcal{N}^2$ denote the set of all OD pairs with positive demand. In our model, travelers between an OD pair choose the departure time and routes. Denote by d_{rs} the total demand traveling from node r to node s (assumed to be known apriori). Let K_{rs} denote the set of all routes connecting OD pair $[r, s] \in \mathcal{P}$ where each route $k \in K_{rs}$ is an ordered sequence of links appearing from start to end. Let $K = \cup_{[r,s] \in \mathcal{P}} K_{rs}$ be the set of all routes in the network. The flow from node r to node s departing at time t via route $k \in K_{rs}$ is denoted by $h_k(t)$. Below equation defines the flow conservation for each OD pair.

$$d_{rs} = \sum_{t \in T} \sum_{k \in K_{rs}} h_k(t) \forall [r, s] \in \mathcal{P}$$

Next, we describe the dynamic network loading model. Below equation denotes the link occupancy (Figure 5), or the number of vehicles on a given link $l \in \mathcal{L}$ at time $t \in T$, which is the difference between the cumulative arrival and departure curves $A_l(t)$ and $D_l(t)$.

$$o_l(t) = A_l(t) - D_l(t) \forall l \in \mathcal{L}, t \in T$$

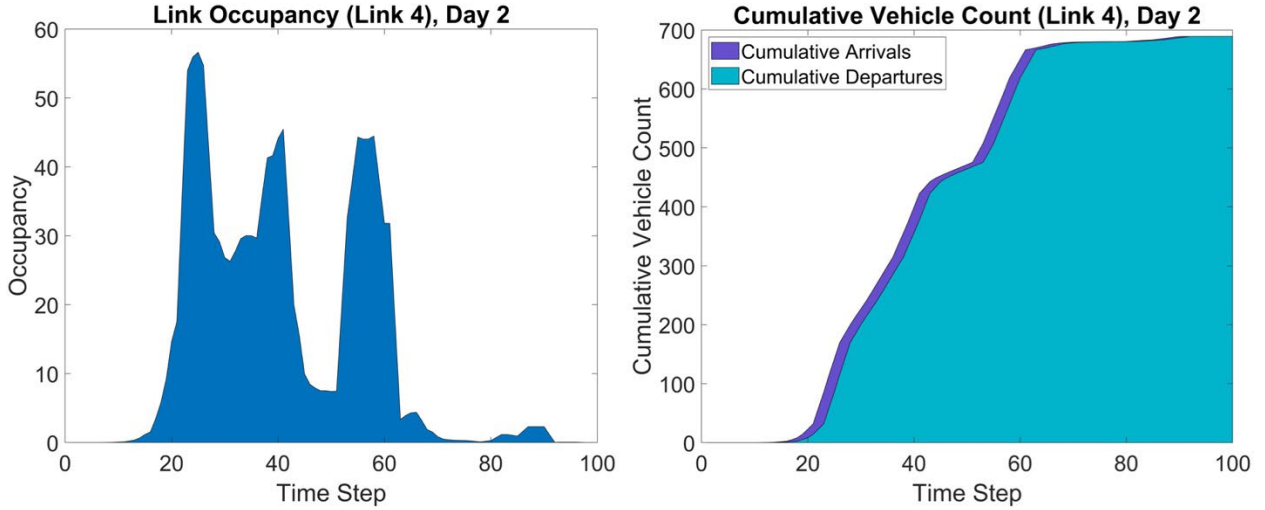


Figure 5 Example link occupancy curve

The density $\rho_l(t)$ on link l at time t is denoted as a function of the number of lanes on the link (denoted by n_l) and the length of the link (denoted by L_l).

$$\rho_l(t) = \frac{o_l(t)}{n_l L_l}$$

This density function can be generalized for any spatial location x measured along the length of a link l at time t , represented as $\rho_l(t, x)$, by taking the limit of the ratio of total time with the total area in the time space diagram as the area of the region becomes infinitely close to zero centered at point (t, x) .

Models for traffic flow determine the variation of density for different times and locations. The Lighthill-Whitham-Richards (LWR) model (Lighthill and Whitham, 1955; Richards, 1956) assumes a deterministic relationship between density and flow expressed as fundamental diagram and denoted by $f_l(\cdot)$ for all links $l \in \mathcal{L}$. Incorporating the conservation of vehicles, the partial differential equation (PDE) is then used to calculate dynamics of density and flow across each link:

$$\partial_t \rho_l(t, x_l) + \partial_x f_l(\rho_l(t, x_l)) = 0 \quad x_l \in [a_l, b_l], \forall t \in T \text{ and } l \in \mathcal{L}$$

where x_l is any point along the length of the link $l \in \mathcal{L}$ with a_l and b_l denoting the start and end points of the link (assuming a parameterized curve that represents a link in two dimensions).

In our model, we assume the flow function $f_l(\cdot)$ in the LWR model is given by a triangular fundamental diagram as shown in Figure 6. This fundamental diagram uses two linear functions to approximate the relationship between flow and density on any given link. The intercept of the two functions is the critical density ρ_l^c for the link, while the jam density ρ_l^{jam} is the location where the function with a negative slope intersects the density axis.

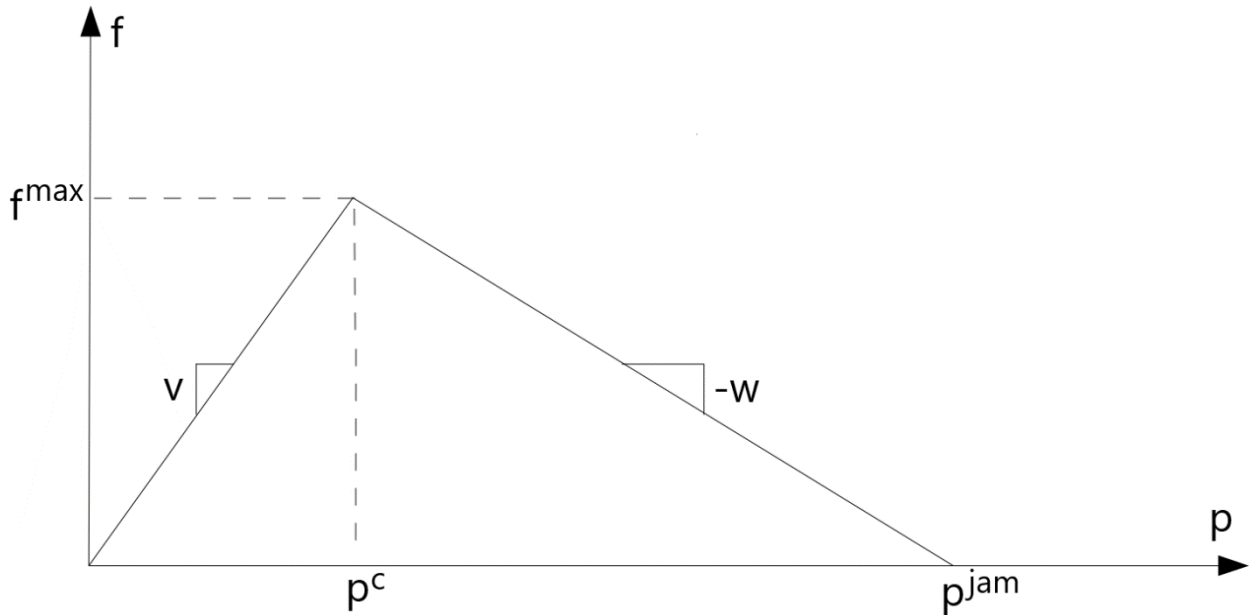


Figure 6 Triangular fundamental diagram

Using the triangular fundamental diagram, the flow for a given density, forward wave speed v , and backward wave speed w is given by below equation (Newell, 1993a; Newell, 1993b; Newell, 1993c).

$$f_l(\rho) = \begin{cases} v\rho & \rho \in [0, \rho_l^c] \\ -w(\rho - \rho_l^{\text{jam}}) & \rho \in [\rho_l^c, \rho_l^{\text{jam}}] \end{cases}$$

To solve the PDE we need to know the time-varying rates of maximum flow that can enter each link (link demand) and the time-varying rates of maximum flow that can exit each link (link supply). The time-varying supply and demand functions for each link, denoted by $S(\rho_l(t))$ and $D(\rho_l(t))$ respectively, can then be approximated using the triangular fundamental diagram (Lebacque and Khoshyaran, 2013), where C is the link capacity.

$$D(\rho_l(t)) = \begin{cases} v\rho_l(t) & \rho < \rho_l^c \\ C & \rho \geq \rho_l^c \end{cases}$$

$$S(\rho_l(t)) = \begin{cases} C & \rho < \rho_l^c \\ -w(\rho_l(t) - \rho_l^{\text{jam}}) & \rho \geq \rho_l^c \end{cases}$$

The flow model on each link can be extended to networks with multiple links meeting at junctions, which are nodes with at least one incoming and one outgoing link (Han et al., 2019). Let $\mathcal{J} \subseteq \mathcal{N}$ denote the set of all junctions. For a given junction $n \in \mathcal{J}$, conservation of flow across all links is given by Eq. 8 which can be used as additional boundary condition to solve the combined PDEs for each incoming and outgoing link:

$$\sum_{m \in M_n} f_m(\rho_m(t, b_m)) = \sum_{q \in Q_n} f_q(\rho_q(t, a_q)) \quad \forall t \in T, n \in \mathcal{J}$$

where $M_n \subset \mathcal{L}$ and $Q_n \subset \mathcal{L}$ are the sets of all incoming and outgoing links to junction n , respectively, b_m is the end of an incoming link m , and a_q is the start of an outgoing link q (Recall the parameterization on a link curve using spatial variable $x \in [a_l, b_l]$ from Eq. 4). To prevent the confusion, subscripts m or q are used in this paper to indicate the association with inlink m or outlink q .

Various junction dynamics determine how flows split at each junction. In our model, we consider a path-based DNL that tracks flow on each path. The decision making of users who pass through each junction are considered in Figure 6 to calculate the actual supply and demand on each of the connecting links. This is accomplished by calculating the proportion of users on an incoming link $m \in M$ who will select the outgoing link $q \in Q$. Given the cumulative arrival and departure curves, it is possible to determine an entry time for each link $\tau_m(t)$ based on the exit time (t) for a link m . Let $\gamma_{m,k}(t, b_m)$ denote the proportion of flow leaving link m from its exit point b_m along route k at time t . Following the first-in-first-out principle and using the link entry time for a given exit time, the proportional contribution of an individual path flow to the total flow on a given link at time t can be estimated as follows:

$$\gamma_{m,k}(t, b_m) = \gamma_{m,k}(\tau_m(t), a_m)$$

In other words, the proportion of flow leaving link m along path k at time t is equal to the proportion of flow entering link m at time $\tau_m(t)$. The sum of these proportions on link m over each path containing two connected links m and q gives the total proportion $\alpha_{m,q}(t)$ of flow entering link q from link m at time t as shown in Figure 7. That is,

$$\alpha_{m,q}(t) = \sum_{\forall k \ni m,q} \gamma_{m,k}(t, b_m)$$

Path 1 $\ni [1, 2]$
Path 2 $\ni [1, 3]$

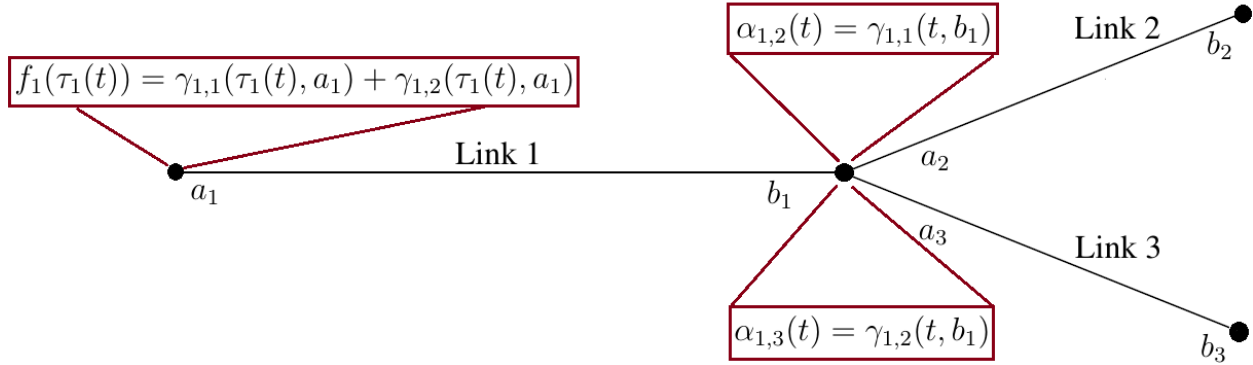


Figure 7 junction dynamic example

A distribution matrix $\mathcal{A}^n(t)$, for a junction $n \in \mathcal{J}$ satisfying conservation of flow in Eq. 8, is then constructed to track the distribution of flows between incoming and outgoing links (Han et al., 2019).

$$\mathcal{A}^n(t) = \{\alpha_{m,q}(t)\} \forall m \in M_n, q \in Q_n, n \in \mathcal{J}$$

The non-junction nodes such as source nodes with no incoming links and sink nodes with no outgoing links consider simplified traffic dynamics. Sink nodes are assumed to have infinite sink capacity allowing the flow on routes terminating at the sink node to exit. On contrary, source nodes may not be able to load the entire demand if the outgoing links experience queue spillback. A point-queue model is used to account for the dynamics at origin nodes (which includes source nodes or junctions that also act as origins). We skip the details for brevity and refer the reader to Han et al. (2019) for more details. In the following section, the uninformed and informed driver models are introduced.

Uninformed Driver Model

We model the day-to-day behavior of drivers after a disruption to the network where drivers adapt their departure time and route choice. Let \mathcal{D} denote the set of days post disruption indexed by d ranging from $1, 2, \dots, |\mathcal{D}|$. The update dynamics of departure time and route choice for uninformed drivers is governed by an iterative structure where travelers adapt their routes to converge to the new post-disruption equilibrium. We approximate this dynamic using a multinomial Logit model described next.

First, to circumvent exponentially high number of routes, we narrow the set of possible routes over which travelers consider updating their routes. We define canonical routes as the set of routes that deviate from the fastest path (i.e., minimum travel time path) within a specified

tolerance. For a traveler departing from O-D pair $[r, s] \in \mathcal{P}$ at time $t \in T$, the set of canonical routes is denoted by $\mathcal{R}_{rs}(t)$ and is defined as following:

$$\mathcal{R}_{rs}(t) = \left\{ k \mid k \in K_{rs}, \frac{TT_k(t) - TT_{rs}^*(t)}{TT_{rs}^*(t)} \leq \theta \right\}$$

where $TT_k(t)$ is the travel time on route k for departure time t , $TT_{rs}^*(t)$ is the travel time on the time-dependent shortest path connecting O-D pair $[r, s] \in \mathcal{P}$ for departure time $t \in T$, and θ is the driver's perception deviance. We assume θ to be fixed across all travelers. We note that the canonical route set is time-dependent since shortest path may be different for different departure times.

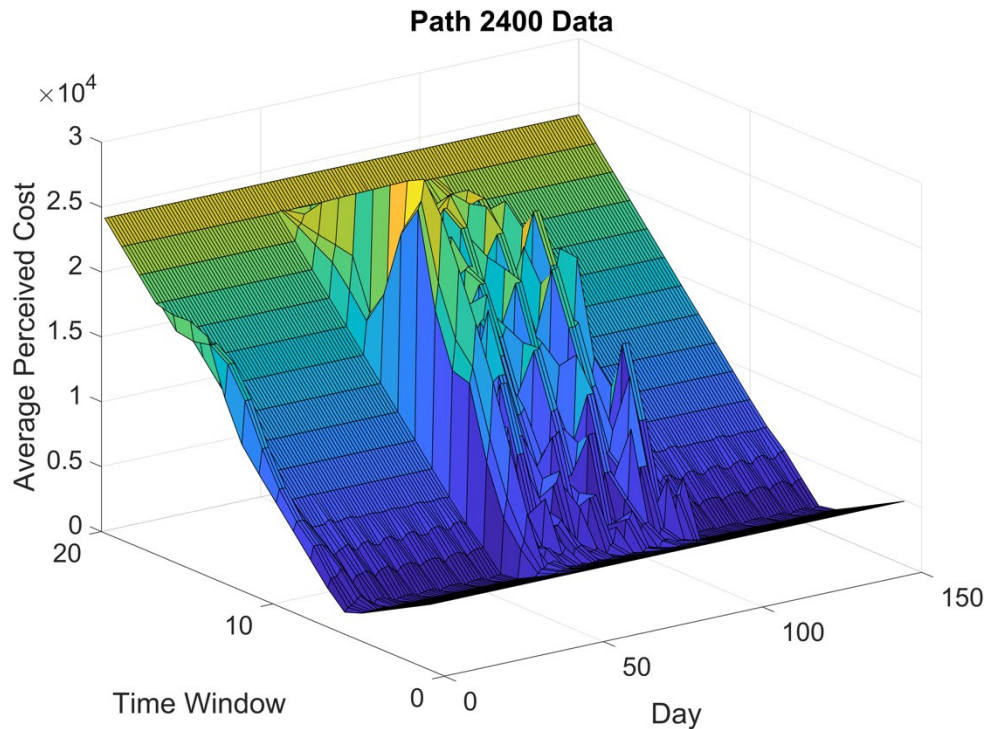


Figure 8 Sioux Falls Network perceived cost in seconds for path 2,400, out of 6,180 paths, for each day and departure time window

Building on the BRDUE model proposed by (Han et al., 2015), we update the route and departure time decisions for uninformed drivers using a Multinomial Logit Model (Mlogit). Let $(k, t)_d$ denote the choice tuple representing the route and the departure time on day $d \in \mathcal{D}$. After executing the select choices on a given day, travelers update their choices $(k, t)_{d+1}$ for the next day using the MLOGIT model.

The utility of a choice is approximated using the perceived cost (Figure 7) of each route and departure time choice for every O-D pair. We assume homogeneity across all travelers between an origin-destination pair.

The perceived cost for each route and departure time, in terms of both travel time and schedule delay (early or late arrival), is calculated in Eq. 13

$$PC_k(t) = TT_k(t) + SCD_k(t) \quad \forall k \in K, t \in T$$

where $SCD_k(t)$ is the schedule delay cost for path k and departure time t , given by Eq. 14,

$$SCD_k(t) = \begin{cases} \phi_e(AT_k(t) - TA_{rs}) & \text{if } AT_k(t) \leq TA_{rs} \\ \phi_l(AT_k(t) - TA_{rs}) & \text{if } AT_k(t) > TA_{rs} \end{cases} \quad \forall k \in K_{rs}, [r, s] \in \mathcal{P}, t \in T$$

where $AT_k(t) = t + TT_k(t)$ is the actual arrival time at the destination for route k and departure time t , TA_{rs} is the desired arrival time for all travelers associated with the OD pair $[r, s]$ (a single value assumed to be known apriori for each OD pair), ϕ_e is the coefficient of early arrival penalty, and ϕ_l is the coefficient of late arrival penalty. Eq. 13 can now be incorporated into the Mlogit model.

The Mlogit model estimates the probability of choosing an alternative given the utilities across all alternatives. Let C_{rs} be the set of all alternatives for all travelers across an OD pair $[r, s] \in \mathcal{P}$, defined as follows:

$$C_{rs} = \{(k, t) \mid k \in \mathcal{R}_{rs}(t), t \in T\}$$

For the Mlogit model, the utility of an alternative $(k, t) \in C_{rs}$ is given by $U_{(k,t)} = -PC_k(t) + \varepsilon_{(k,t)}$, where $\varepsilon_{(k,t)}$ are the error terms associated with the utilities that are assumed to be independent and identically distributed as a Gumbel distribution with a scale parameter $\theta > 0$ and location parameter assumed to be 0. Given the assumptions, the probability of choosing alternative $(k, t) \in C_{rs}$ for travelers between OD pair $[r, s]$ is given by:

$$\begin{aligned} \mathbb{P}_{(k,t)} &= \mathbb{P} \left(U_{(k,t)} > \max_{\substack{(k',t') \in C_{rs} \\ (k',t') \neq (k,t)}} U_{(k',t')} \right) \\ &= \frac{\exp(-\theta PC_k(t))}{\sum_{(k'',t'') \in C_{rs}} \exp(-\theta PC_{k''}(t''))} \end{aligned}$$

and the path flows for a given departure time is computed as:

$$h_k(t) = d_{rs} \mathbb{P}_{(k,t)} \quad \forall (k, t) \in C_{rs}, [r, s] \in \mathcal{P}$$

To model the boundedly-rational behavior of travelers, we consider an indifference band Δ that increases the utility of current alternative thus increasing the likelihood that the traveler continues to stay on the currently chosen alternative over the next day. Adding a superscript d denoting the day of travel, we denote by $h_k^d(t)$ the number of travelers choosing route k at time t on day d . We can then update the flow on next day $d + 1$, by considering the current flow on alternative (k, t) that continues to stay with the same alternative, and the flow from all other alternatives (k', t') that switch to the alternative (k, t) .

Equation 17 shows the update of flow from one day to the next.

$$h_k^{d+1}(t) = h_k^d(t) \mathbb{P}_{(k,t) \leftarrow (k,t)} + \sum_{\substack{k',t' \in C_{rs} \\ (k',t') \neq (k,t)}} h_{k'}^d(t') \mathbb{P}_{(k,t) \leftarrow (k',t')}$$

where $\mathbb{P}_{(k,t) \leftarrow (k,t)}$ is the probability that travelers choosing alternative $(k, t) \in C_{rs}$ will continue with the same alternative on the next day, computed as:

$$\mathbb{P}_{(k,t) \leftarrow (k,t)} = \frac{e^{(-\theta \times (PC_k(t) - \Delta))}}{e^{(-\theta \times (PC_k(t) - \Delta))} + \sum_{\substack{c'',t'' \in C_{rs} \\ (k'',t'') \neq (k,t)}} e^{(-\theta \times PC_{k''}(t''))}}$$

and $\mathbb{P}_{(k,t) \leftarrow (k',t')}$ is the probability that travelers choosing alternative $(k', t') \in C_{rs}$ will switch their alternative to (k, t) on the next day, computed as:

$$\mathbb{P}_{(k,t) \leftarrow (k',t')} = \frac{e^{(-\theta \times PC_k(t))}}{e^{(-\theta \times (PC_{k'}(t') - \Delta))} + \sum_{\substack{(k'',t'') \in C_{rs} \\ (k'',t'') \neq (k',t')}} e^{(-\theta \times PC_{k''}(t''))}}$$

It is easy to verify that if $\Delta = 0$, then $\mathbb{P}_{(k,t) \leftarrow (k',t')} = \mathbb{P}_{(k,t) \leftarrow (k,t)} = \mathbb{P}_{(k,t)}$,

Informed Driver Model

Informed drivers in the presented model are given route suggestions that minimize a cost function representing the total system cost. These users seek to reduce congestion faced by all other drivers in the network, but without noticeably penalizing themselves. Such a cost function needs to consider both the system-level cost and the cost to the user when selecting a path and departure time.

DSO Computation

Let $\mathbf{h} = \{h_k(t) \mid k \in K, t \in T\}$ denote the departure-rate pattern as a vector of all path flows at different departure times. The DSO formulation is defined using the following optimization problem (Doan and Ukkusuri, 2015)

$$\min_{\mathbf{h}} \left(\text{TSC} = \sum_{k \in K} \sum_{t \in T} h_k(t) \times PC_k(t) \right)$$

subject to the following constraints:

$$\begin{aligned} \sum_{t \in T} \sum_{k \in K_{rs}} h_k(t) &= d_{rs} \quad \forall [r, s] \in \mathcal{P} \\ h_k(t) &\geq 0 \quad \forall k \in K, t \in T \end{aligned}$$

where $h_k(t)$ is the departure rate, and $PC_{k,t}$ is the perceived cost for route k at time t , and TSC is the total system cost.

As shown in Doan and Ukkusuri (2015), a departure rate pattern \mathbf{h} is a DSO solution if and only if it is equilibrated based on the corresponding path marginal cost (PMC). The PMC is defined as the increase in total system cost incurred when an additional unit of flow is added to the departure rate pattern $h_k(t)$. The PMC for route k at time t is calculated in Eq. 23

$$PMC_{k,t} = \frac{\partial \text{TSC}}{\partial h_k(t)} = PMC_{k,t}^{TT} + PMC_{k,t}^{SCD} + PC_k(t)$$

where $PMC_{k,t}^{TT}$ is the change in travel time cost for all other users caused by additional flow on route k at time t , $PMC_{k,t}^{SCD}$ is the change in schedule delay cost for all other traffic caused by the additional flow on route k at time t , and $PC_k(t)$ is the perceived cost for an individual on route k at time t (Eq. 13).

Naively using a DNL algorithm to calculate the PMC for each path and departure time is computationally demanding for anything beyond small-scale toy networks with the limited route and departure time choices. For a set of all time periods, the naive method requires $|\mathcal{P}| \times |T|$ DNL solutions per DSO iteration.

We approximate the $PMC_{k,t}^{TT}$ using the Bureau of Public Roads (BPR) function since solving the exact path marginal cost is complex due to the non-linear nature of the DNL procedure. While actual DNL is used for daily simulation of revised change in flow, the cost incurred by each traveler's route and departure time choice is estimated with revised BPR function.

Let's assume that an estimate for the travel time on route k at departure time t can be calculated using the BPR function (24) (Bureau of Public Roads (BPR), 1964)

$$TT_k(t) \approx t_{0,k} \times \left[1 + \alpha \left(\frac{h_k(t)}{C_k} \right)^\beta \right]$$

where $t_{0,k}$ is the free flow travel time (defined as the sum of free flow travel time on path links), $h_k(t)$ is the flow (e.g. veh/hr) on route k at time t , C_k is the capacity of route k , and α and β are parameters. We define C_k to be the minimum capacity across all links along the path.

While the congested links and time of congestion are computed from DNL, we consider the revised BPR to approximate the change in cost to all other paths due to change in flow on path k . To compute the impact of one unit of flow with and without the presence of congestion, we find all the paths that go through congested links in route k and iterate through all of the links in route k . Once the value of $PMC_{k,t}^{TT}$ is approximated, the revised destination arrival time is estimated at the destination of route k for a departure time t , and the new value of $PMC_{k,t}^{SDC}$ is approximated using Eq. 14 as before.

Substantial computational improvements are made by only calculating PMC for paths and times which incur congestion, and which propagate congestion onto other paths and departure times (Doan and Ukkusuri, 2015). This is accomplished by avoiding computing PMC for all uncongested paths and times, since these paths and times are assumed to be traversed at the free flow travel time and have no marginal cost on other paths or departure times. In addition, no PMC calculations are required for other paths and departure times which are unaffected by congestion on a given path at a given time. As shown in the triangular fundamental diagram (Eq. 5), there is no impact of an additional vehicle below critical density for the link. Using these methods, the total number of paths and departure times requiring PMC calculation is minimized for a given spatiotemporal distribution of congestion in the network. After PMC for each path is solved, informed drivers make an updated decision using the Informed Driver Mlogit Model (IDMM) described in the next subsection, then the DNL model is executed to generate a new congestion pattern based on the decisions of informed drivers.

Informed Driver Mlogit Model (IDMM)

Finding DSO for informed drivers requires multiple iterations of route and departure time decisions. Unlike the MSA and quadratic programming models presented by Doan and Ukkusuri (2015), in each subiteration i of DSO computations route and departure time decisions for informed drivers are made using the Mlogit model. Mlogit models are used for alternative-invariant problems, meaning that the regressor does not vary over the alternatives but does vary over the individual. Since the PMC already accounts for the effect that selecting an alternative has on all other alternatives and presents it as a cost which varies only over the individual, the IDMM described in this section can be treated as alternative-invariant.

Informed drivers also consider route choice over a limited canonical set of routes as defined in Eq. 12. For the informed drivers, the utility of an alternative $(k, t) \in C_{rs}$ is given by $U_{(k,t)} = -PMC_{k,t} + \varepsilon_{(k,t)}$. The PMC for each path k and departure time t available to the O-D pair p is calculated for use in the IDMM. As in the previous section, the selection of base alternative for each solution is sequentially selected from the set of paths between the O-D pair and the set of possible departure times.

$$PMC_{k,t} = PC_k(t) + PMC_{k,t}^{TT} + PMC_{k,t}^{SCD}$$

where $PMC_{k,t}^{SCD}$ is the sum of schedule delays (Eq. 14) for all other paths and departure times when 1 additional unit of flow is added to path k at time t , $PMC_{k,t}^{TT}$ is the cost in terms of travel time for all other paths and departure times when 1 additional unit of flow is added to path k at

time t , and $PMC_k(t)$ is the perceived cost of current flow on path k at time t . Therefore, $PMC_{k,t}$ is the marginal cost of path k at time t on all other paths and departure times. We can add travel time without schedule delays because if drivers arrive within the desired arrival time window, there is no penalty, however, if not, those will be in the later time window. Having many drivers departing at the same time as an aggregate will incur congestion, which we want to avoid.

The update of flow from one iteration to the next is governed by the IDMM model. For each OD pair $[r, s] \in \mathcal{P}$, the model computes the probability of switching from all other route-departure time tuples $(k', t') \in C_{rs}; (k', t') \neq (k, t)$ to a given alternative tuple $(k, t) \in C_{rs}$. The total probability of choosing route k and departure time t in the next iteration also includes the proportion of drivers who already selected route k at time t and choose not to detour or adjust their departure time. Similarly to the uninformed model, a constant scaling parameter $\theta_2(0.04)$ is used for distribution of utility errors, along with the BR switching threshold $\Delta_2(800 \text{ s})$, which still applies to informed drivers since not all drivers will be convinced to switch when provided with a predictive alternate route.

Path flow update from iteration i to $i + 1$ for computing DSO is computed as follows. First, adding a superscript i, DSO denoting the subiteration of DSO computation, we denote by $h_k^{i, DSO}(t)$ the number of travelers choosing route k at time t in DSO iteration i . We can then update the flow on next iteration $i + 1$, by considering the current flow on alternative (k, t) that continues to stay with the same alternative, and the flow from all other alternatives (k', t') that switch to the alternative (k, t) . We assume that the uninformed driver flow is unaffected and remains constant in the background for each DSO iteration.

Equation shows the update of flow from one iteration to the next.

$$h_k^{i+1, DSO}(t) = h_k^{i, DSO}(t) \mathbb{P}_{(k,t) \leftarrow (k,t)}^{DSO} + \sum_{\substack{(k', t') \in C_{rs} \\ (k', t') \neq (k,t)}} h_{k'}^{i, DSO}(t') \mathbb{P}_{(k,t) \leftarrow (k', t')}^{DSO}$$

where $\mathbb{P}_{(k,t) \leftarrow (k,t)}^{DSO}$ is the probability that travelers choosing alternative $(k, t) \in C_{rs}$ will continue with the same alternative in the next DSO iteration, computed as:

$$\mathbb{P}_{(k,t) \leftarrow (k,t)}^{DSO} = \frac{e^{-\theta_2 \times (PMC_{k,t} - \Delta_2)}}{e^{-\theta_2 \times (PMC_{k,t} - \Delta_2)} + \sum_{\substack{(k'', t'') \in C_{rs} \\ (k'', t'') \neq (k,t)}} e^{-\theta_2 \times PMC_{k'', t''}}}$$

and $\mathbb{P}_{(k,t) \leftarrow (k', t')}^{DSO}$ is the probability that travelers choosing alternative $(k', t') \in C_{rs}$ will switch their alternative to (k, t) in the next DSO iteration, computed as:

$$\mathbb{P}_{(k,t) \leftarrow (k',t')}^{\text{DSO}} = \frac{e^{(-\theta_2 \times \text{PMC}_{k,t})}}{e^{(-\theta_2 \times (\text{PMC}_{k',t'} - \Delta_2))} + \sum_{\substack{(k'',t'') \in C_{rs} \\ (k'',t'') \neq (k',t')}} e^{(-\theta_2 \times \text{PMC}_{k',t'})}}$$

The iterative process of shifting travelers along different alternatives continues until convergence criteria is met. While convergence guarantees are hard to establish, for our experiments, we terminate the iterative process after a fixed number of DSO iterations.

Parallelization

An additional convenient property of the WD DSO methodology is that it is easily parallelized, allowing further computational improvements over the serial method. The ease of parallelization comes from the fact that each calculation of PMC only considers the effect of one path and departure time on all other paths and departure times. Each PMC calculation is independent of other PMC calculations. Therefore, parallelization can be applied to make the problem more computationally tractable on the Sioux Falls Network with 6,180 paths and 100 departure time windows.

Without using parallelization and other methods to reduce the number of required DNL solutions, solving the problem requires sequentially executing the DNL algorithm 618,000 times per DSO iteration, with a large number of DSO iterations required to converge using MSA.

Simulations were performed using an Intel[®] i7-8700K 6 core, 12 thread CPU running at 4.3GHz continuously on all cores and 32 GB of DDR 4 memory at 3200MHz implemented in MATLAB[®] (MATLAB, 2019). With parallelization on a 12 threads CPU, the expected speedup relative to a single core can be estimated using Amdahl's Law (Amdahl, 1967)

$$S(s) = \frac{1}{(1-p) + \frac{p}{s}}$$

where S is the speedup, s is the number of threads, and f is the fraction of the algorithm which benefits from parallelization. Figure 9 shows the relationship between the number of processors and the speedup, and the fraction of parallelizable code and the speedup, respectively.

As a result of several simulation, observed speedup of 5.3 by using 12 threads provides us the 0.886 as the fraction of the algorithm which benefits from parallelization.

Original computational times were projected to take approximately 30 h based on the number of iterations required and several hours of testing with smaller numbers of DSO iterations. Compute times were first reduced through the careful use of constraints that avoid computations for non-congested routes to approximately 8 h. After parallelization the computational time required to generate a solution averaged approximately 1.5 h.

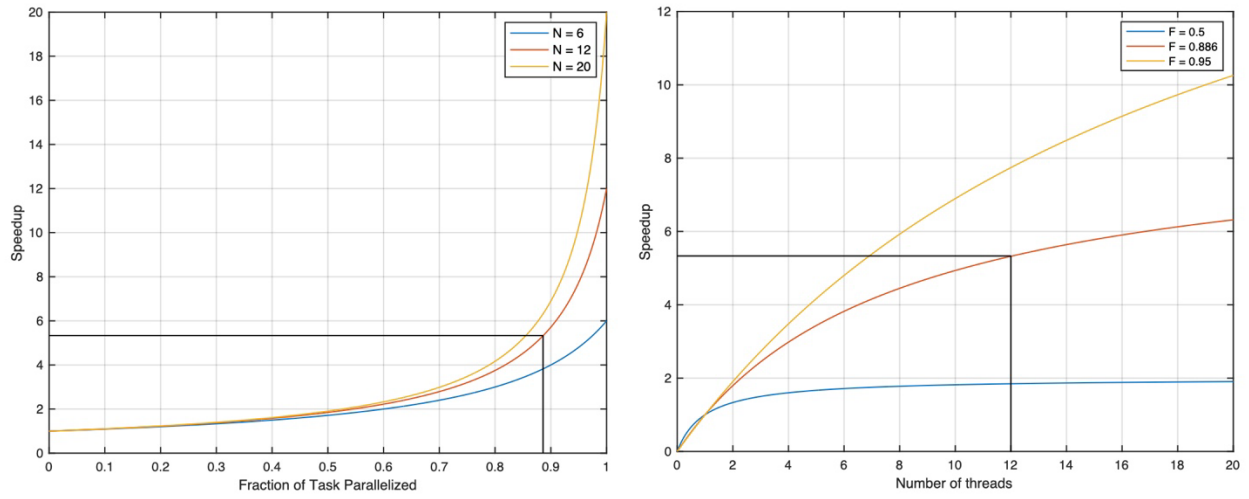


Figure 9 Effect of varying the number of threads and the fraction of parallelizable code on speedup

Results

Experimental Design and Procedure

The experiment is conducted on the Sioux Falls Network using a DTA algorithm by extending the DTD BRDUE package developed by Han et al. (2019) with the addition of aWD DSO algorithm and another group of drivers who use a competing WD DSO strategy. The Sioux Falls Network contains 24 nodes, 76 links, 528O-Dpairs, and 6,180 routes. There are 20 departure time windows containing 5 departure times each, for a total of 100 possible departure times. Figure 10 shows three possible paths from Node 1 to Node 4 in the Sioux Falls Network, which are paths 5, 6, and 7 in the list of 6,180 routes. Two of these paths contain shared links, and users choosing paths 5 or 6 will contribute to congestion on links 1 and 4. Therefore, users choosing path 5 can worsen congestion for users on path 6, and the opposite is also true. Users choosing path 7 should not contribute to congestion for paths 5 and 6 because there are no shared links in the paths.

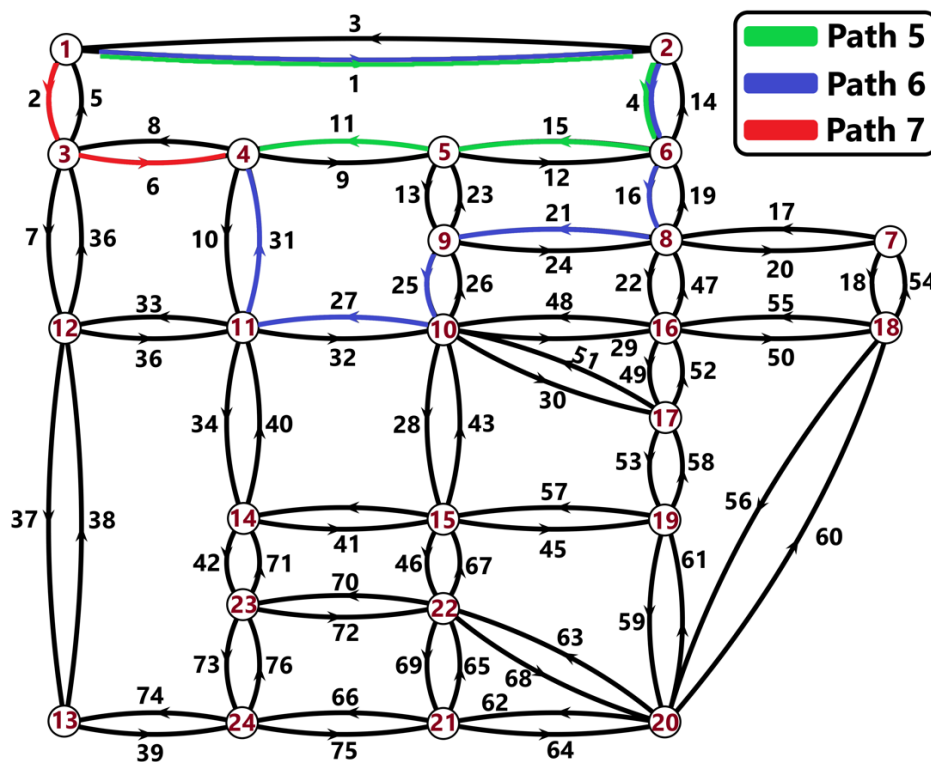


Figure 10 Example of the available routes between nodes 1 and 4 in the Sioux Falls Network.

For the first day, demand for each O-D pair at each departure time is initialized and the DNL algorithm calculates the delay for each route and departure time. Two groups of drivers are initialized by multiplying total demand by a user defined informed driver fraction. If this fraction is 1/5, then 80% of the demand will be assigned to Group 1 and 20% will be assigned to Group 2. Group 1 drivers are uninformed and work toward DTD BRDUE, while Group 2 drivers are informed and push the network toward WD DSO equilibrium. Informed and Uninformed demand

are always summed as an input to the DNL procedure, but the groups make separate route and departure time choices, while switching to predicted alternate routes will be based on the bounded rationality of drivers. The first run through the DNL procedure generates the expected delay for the day based on the initialized O-D demand without the informed-decision strategy. Using the anticipated delay, the marginal cost of each route is estimated as the increase in the cost of each route for a small change in the OD demand for the associated route's OD pair. Informed drivers are recommended routes and departure times using the marginal cost of each route such that the total system cost is minimized. The new route and departure time choices for the informed group of drivers are the informed group demand. This demand is summed with the uninformed group demand and input into the DNL algorithm to determine the actual route delays for the day.

Scenario Design

The simulation is run for two consecutive days, with the first day representing a perturbation in O-D demand. Uninformed users lack the ability to predict the effects of this perturbation and thus create severe delays on the first day of the perturbation. Additionally, once the perturbation is removed, uninformed drivers require additional time to return to their previous behavior patterns. The presented model is expected to perform best during these perturbations; however, if no significant congestion is present, then most informed drivers will not switch routes because the opportunity for congestion reduction is minimized and the network will approach a BRDUE condition.

Figure 11 display average travel time and effective path delay after a 150 day simulation for uninformed drivers. Because daily route choices are influenced by the weighted experience of the past 3 days and its tasks for travelers to adapt to a new equilibrium, this research focuses specifically on the transition between the presence of perturbations and after removal of perturbations. We focus on perturbations caused by disruption such as random incidents, traffic crashes, and work zones, having an impact to cause a change in travelers' route choices. In the first 50 days, the incident rate is low, and the uninformed drivers quickly reach a BRDUE condition after several days. During the second 50 days, a period of daily perturbations is caused by high incident rates. As shown in samples in the green circle in Figure 10, the uninformed users are unable to adapt to these perturbations, because their daily route choices are dictated by the weighted experience of the past 3 days. The final 50 days show a return to the low incident rate; however, the uninformed drivers require several days to adjust before again achieving a BRDUE condition, which is the focus of this study. The effects of the informed decision are highlighted on the day when the perturbation occurs and the next day when the memory still remains. While planned construction sites will provide us enough time to compute long-term dynamics of the system, updates on short-term dynamics from random event will be challenging. We are not running this computationally demanding simulation in real-time, but the app provides the already simulated information in real-time. The online update and real-time validation/ correction of travel time is outside of the scope of this study.

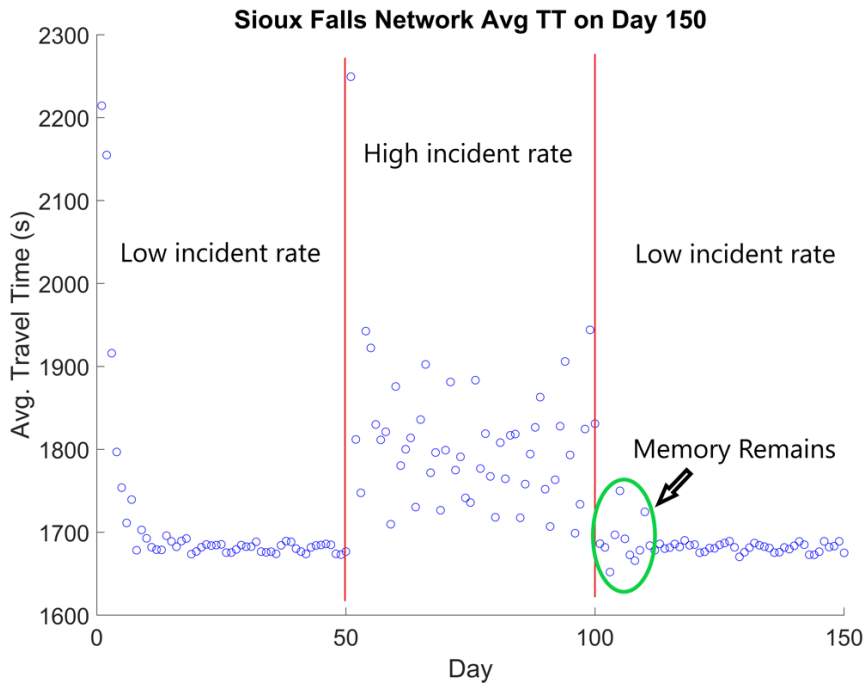


Figure 11 Sioux Falls Network average travel time for uninformed drivers seeking BRDUE.

Given an initial departure rate on the Sioux Falls Network, the effects of varying the fraction of informed drivers on network congestion, O-D gap, and average travel time are considered. The informed drivers make within-day decisions which reduce the congestion caused by uninformed drivers who are following the DTD BRDUE model. The O-D gap is defined as the difference between the maximum and minimum travel time TT for each path k between O-D pair p , as shown in Eq. 30

$$ODgap_p = \max_{\forall k \in p} TT_k - \min_{\forall k \in p} TT_k.$$

Starting from the initial O-D demand, the initial departure rate is determined. This departure rate can be considered as a substantial perturbation from the equilibrium state of the system e.g., even when 20% of drivers on a path with congestion are informed. Figure 12 shows the Day 1 congestion when 20% of the users are informed and switch their route and departure time in order to reduce congestion on all other paths. The perturbation occurs on Day 1 and uninformed users decide to switch their route and departure time choices on Day 2, based on their perceived travel times for the previous day. If no additional perturbations occur, a system of uninformed users will reach a stable BRDUE equilibrium after several days; however, within day delays will occur prior to the system equilibrating. This paper focuses on the within-day transition of traffic state on Day 1 and day-to-day transition of traffic state on day 2, with informed and uninformed decision making strategy. For uninformed drivers, it is expected to take several days to realize the removal of the perturbation in the first day. The departure rates for Day 1 are input to the DTD BRDUE DNL algorithm. This DNL algorithm generates the predicted delay for the network given the initialized demand, assuming that all departures seek DTD BRDUE, as shown in Figure 12.

In this scenario, the perturbation is caused by a large number of drivers departing within a short period of time Figure 13A. The network does not have sufficient capacity for this number of departures and the significant delays shown in Figures 13B,E will be incurred unless some drivers change their route and departure time choices. Many of the drivers whose departure time is $DT > 70$ will not complete their trip prior to the end of the final departure time window. This is indicated by the constant delay values for departure times of $70 < DT \leq 100$ on most of the congested paths.

The predicted delays are used as an input to the DSO algorithm, which outputs a PMC for each path and departure time. Using the PMC information, the informed driver group makes route and departure time choices which seeks to minimize congestion and delays for all other drivers. The DSO algorithm then outputs a new path departure rate (Figure 11C). The final adjusted delay (Figures 11D,F) for the network on Day 1 is the total contribution of the uninformed group (80% of drivers), which does not change their original route and departure choice, and the informed group (20% of drivers on a path with congestion), who do change their route and departure time choice in order to minimize congestion and delays in the network. Compared with the BRDUE only prediction, the paths with constant delay extending to the final DT window have less delay overall when 20% of informed drivers are rerouted. Additionally, the departure times which will not reach the destination before the final departure time window are moved closer to the final departure time window. The scenario will have 6 days of memory remaining to drivers, with the weight of 0.7, while a total number of days are set to be 2 days to show the effect of informed strategy for the first and second day.

The predicted congestion, represented as average excess travel time, incurred on individual links within the Sioux Falls Network given the initial 100% uninformed departure rate is given by Eq. 31

$$\text{Excess}_{k,t} = TT_{k,t} - FFT_{k,t}$$

where $TT_{k,t}$ is the actual travel time and $FFT_{k,t}$ is the free flow travel time for route k and departure time t . The edge weights in Figures 11E,F represent the capacity for each link, with thicker edges indicating links with greater capacity.

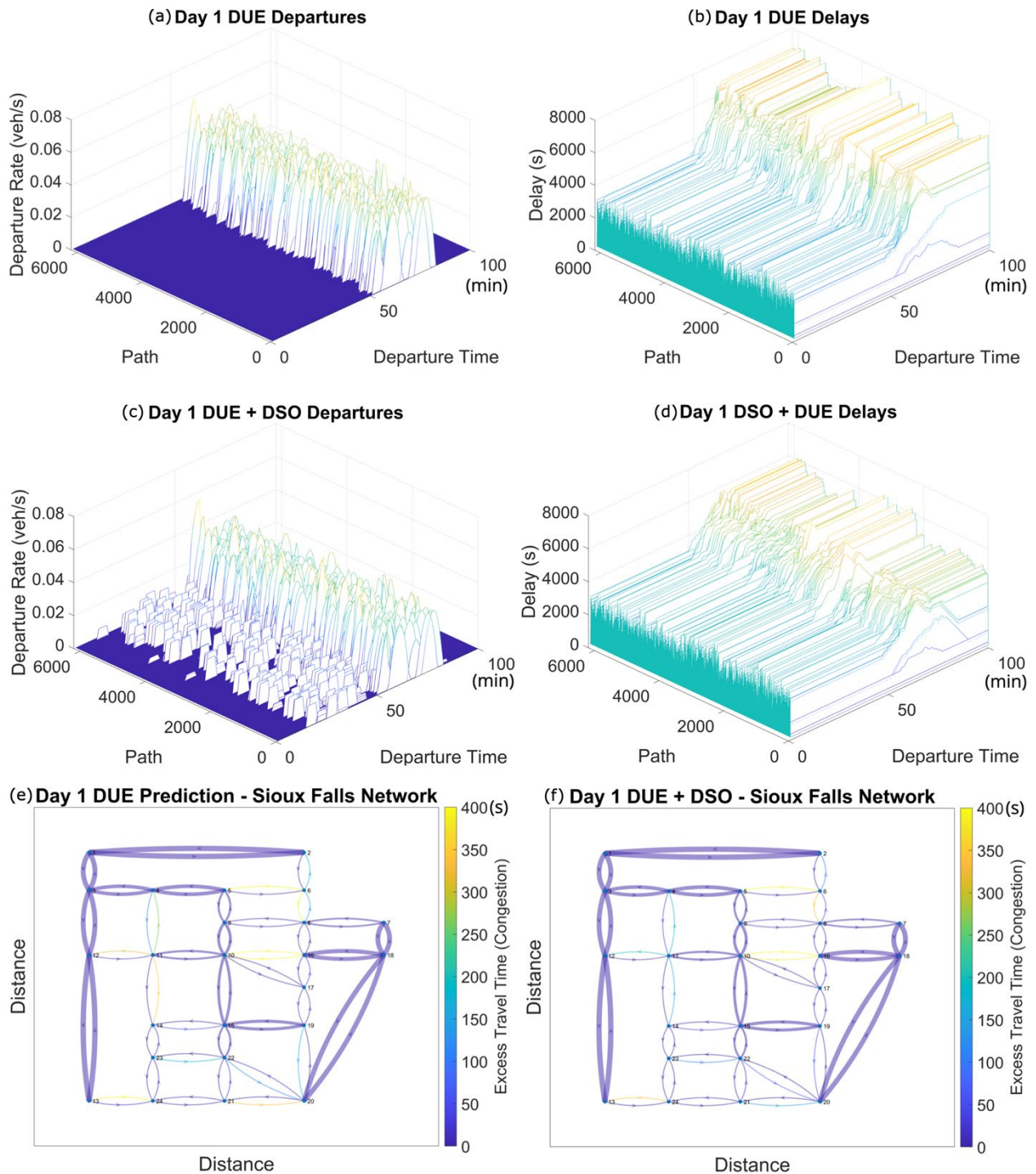


Figure 12 (A) Initial network departures on Day 1 based on initialized O-D demand, prior to informed drivers switching routes. (B) Initial delays on Day 1 based on initialized O-D demand, prior to informed drivers switching routes. (C) Network departures on Day 1 with DSO seeking route choices by the informed driver group. (D) Network delays on Day 1 with DSO seeking route choices by the informed driver group. (E): Uninformed DUE Avg. Excess TT on Day 1. (F) Mixed Objective Avg. Excess TT on Day 1.

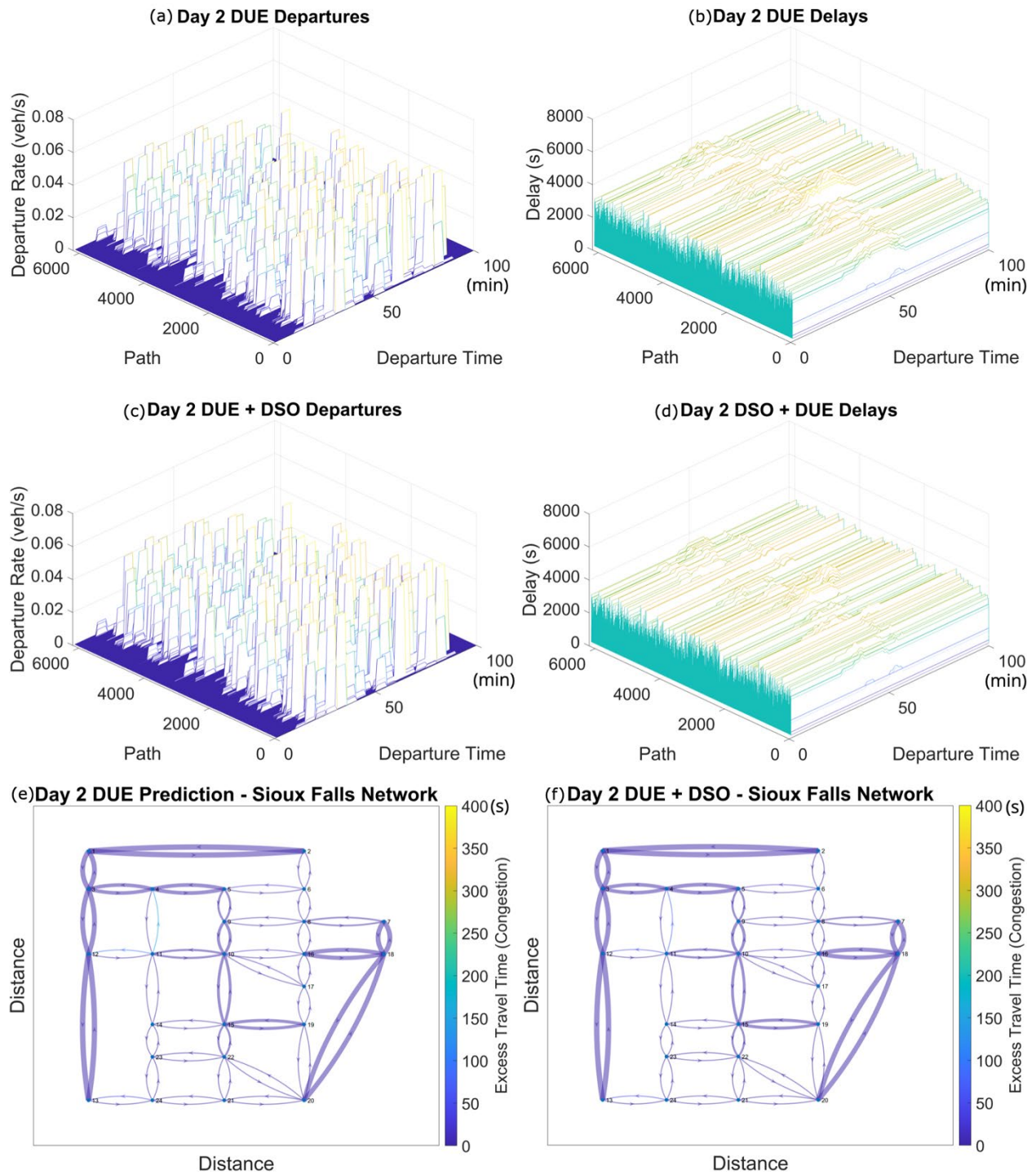


Figure 13 (A) Initial network departures on Day 2 based on initialized O-D demand, prior to informed drivers switching routes. (B) Initial delays on Day 2 based on initialized O-D demand, prior to informed drivers switching routes. (C) Network departures on Day 2 with DSO seeking route choices by the informed driver group. (D) Network delays on Day 2 with DSO seeking route choices by the informed driver group. (E) Uninformed DUE Avg. Excess TT on Day 2. (F) Mixed Objective Avg. Excess TT on Day 2.

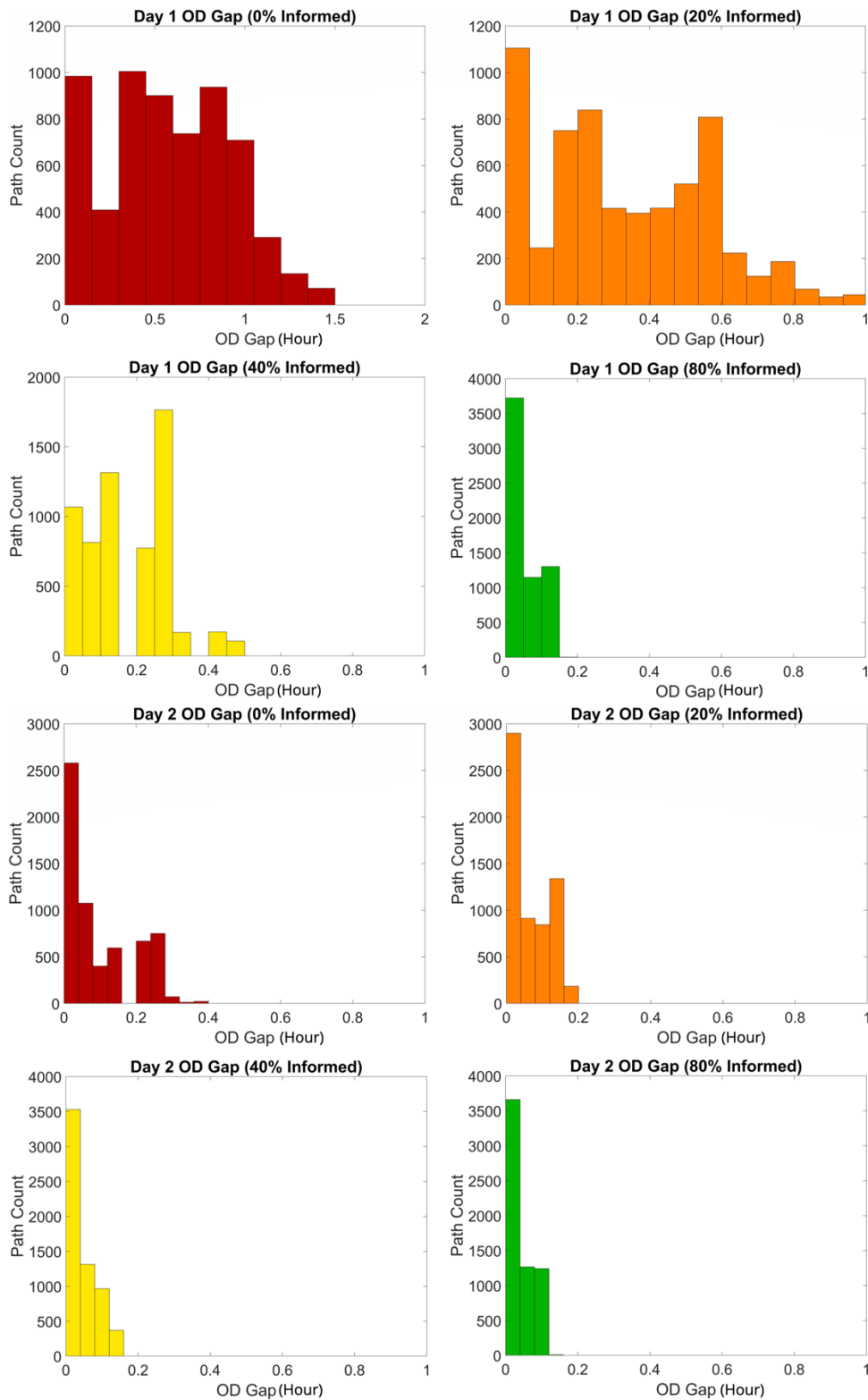


Figure 14 Day 1 and Day 2 O-D Gap for all paths with 0% informed drivers, 20% informed drivers, 40% informed drivers, and 80% informed drivers.

The initial departures for Day 2 assume that all users are seeking BRDUE (Figures 13A,B). This new departure rate pattern (Figures 13C,D) is calculated based on the BRDUE + DSO departure rate pattern from Day 1. Some congestion exists in departure time windows closer to the middle of the evaluation period for Day 2, but because less congestion exists on Day 2, the potential improvement in average travel time by using DSO algorithm is less. Nonetheless, the adjusted departure rates after executing the DSO algorithm further reduce this midperiod congestion noticeably.

Figures 13E,F shows the predicted Day 2 average excess travel time for the Sioux Falls Network if all users seek BRDUE and the average excess travel time for the BRDUE + DSO departure rate pattern. A comparison of the two figures shows a reduction in excess travel time for the two links which were predicted to be congested prior to executing the DSO algorithm.

Figure 14 contains histograms of the travel time gaps in units of hours for Day 1 given 0%, 20%, 40%, and 80% informed drivers. The gaps in each histogram are provided for all paths instead of limiting the gaps to each O-D pair, as this more clearly demonstrates overall network congestion levels for different levels of informed drivers. Figure 13 shows that when 0% of drivers are informed, excess travel times can be as high as 1.5 h with many paths having travel times of 30 min to 1 h. When 20% of drivers are informed, excess travel time is reduced by 30 min and most paths require less than 30 min. Additional improvements occur when 40% and 80% of drivers are informed, with the latter case reducing excess travel time to below 12 min.

Figure 14 shows histograms of the travel time gaps for Day 2 given 0%, 20%, 40%, and 80% informed drivers. On Day 2 when 0% of drivers are informed the maximum travel time is less than 30 min. When 20% of drivers are informed, the maximum travel time is reduced to 12 min. When 40% and 80% of drivers are informed the results improve further in terms of median travel time, with the maximum travel time remaining at approximately 10 min.

Figures 15, 16 compare the average travel time for Day 1 and Day 2 before and after executing the within-day DSO algorithm. Figure 14 shows that as the number of informed drivers increases, the O-D gap for Day 1 decreases significantly. Less improvement is available on Day 2 because the congestion level is much lower due to the adaptations of BRDUE seeking drivers. The red bars in Figure 15 show the expected average travel time given the predicted BRDUE departure rates for Days 1 and 2, while the orange bars show the average travel time with departure rate pattern composed of 80% BRDUE seeking uninformed users and 20% DSO seeking informed users. Similarly, the yellow and green bars show average travel time for 60% BRDUE and 20% BRDUE, respectively. Day 2 BRDUE departure decisions are based on the actual travel times for Day 1, which are the result of the Day 1 BRDUE + DSO departure rate pattern. The results for Day 2 are very similar for each case because the perturbation is now anticipated by BRDUE users' experience on Day 1, leaving only small optimality improvements to be made by informed drivers. In a real-world scenario, each day will present its own unique perturbations and having a percentage of DSO seeking informed drivers who can be rerouted to reduce congestion will benefit the average travel time for all users of the network.

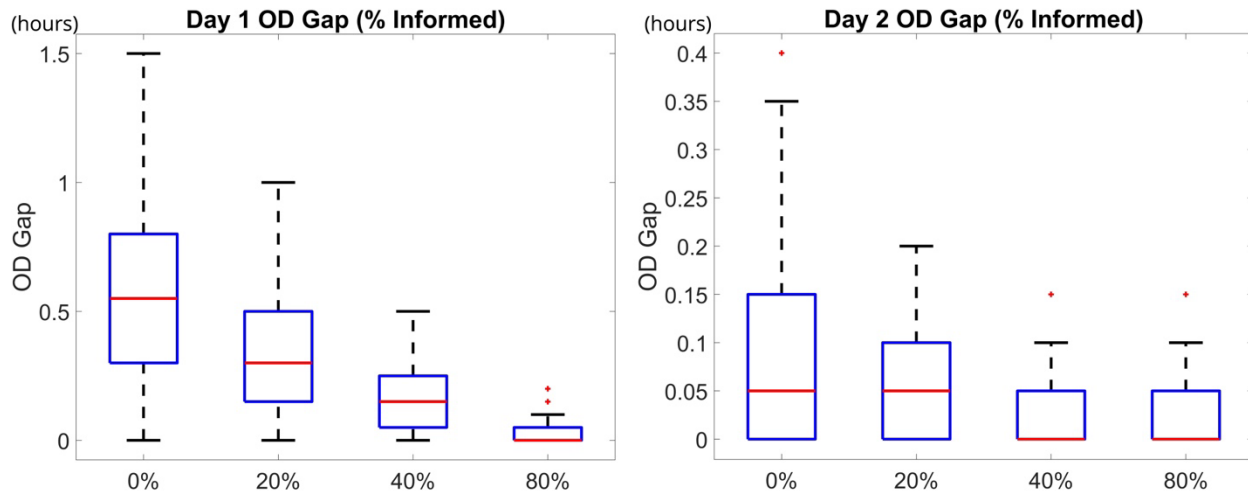


Figure 15 Left: Day 1 O-D gap for all paths under varying fractions of informed drivers. Right: Day 2 O-D gap for all paths under varying fractions of informed

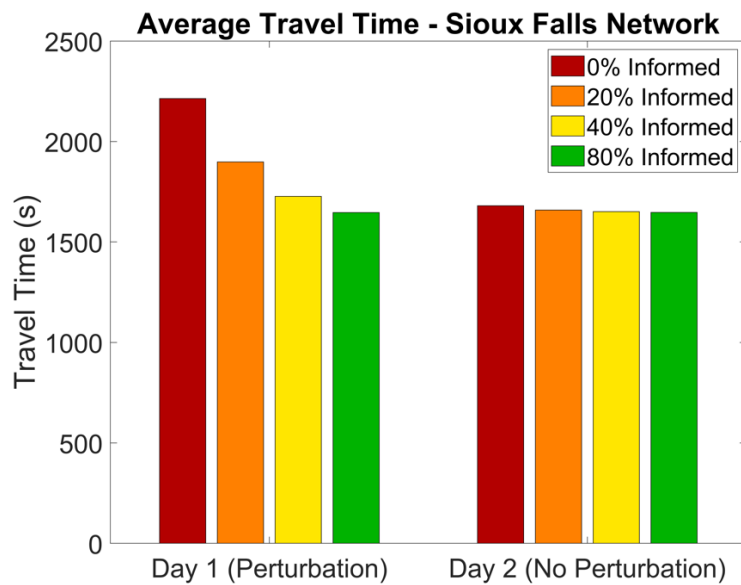


Figure 16 Average Travel Time under varying fractions of informed

Conclusion

This research develops novel techniques for informed and uninformed multi-agent route and departure time choice in midsize city environments. The unstable equilibrium conditions encountered in prior informed driver research are resolved using a strategy which ensures that informed drivers only seek DSO when it is necessary to reduce congestion. Even with a small fraction of informed drivers, results show that congestion can be significantly reduced. Adding parallelization to the DSO algorithm reduces the computational time required from more than

one day to less than 2 hours. Additional speedup is expected by developing the code in a faster programming language and pursuing further multi-core optimization.

The Within-Day delays incurred in a system which follows a DTD BRDUE model can be improved by including informed drivers whose route and departure time choices seek to push the system toward DSO equilibrium. Results show that even with relatively low numbers of drivers seeking Within-Day DSO, significant improvements in average travel time can be obtained. In the cases of severe congestion caused by perturbations, having 20% informed WD DSO seeking drivers can improve the Day 1 average travel time by 59.2% relative to the next day's DTD BRDUE equilibrium solution. As the number of informed drivers increases, the robustness of the system to perturbations improves. Additionally, because informed drivers do not detour unless significant congestion is present, the model always approaches a DTD BRDUE condition for any fraction of informed drivers, rather than having informed drivers naively seek a DSO equilibrium condition.

The Limitation and Future Study

The main limitation of the study is the computational time required to solve the within-day DSO algorithm due to pathbased formulation of BRDUE. For the Sioux Falls network under high congestion, each DSO iteration can take up to 1.5 h to solve. When congestion is less severe, the DSO iterations are faster because fewer paths and departure times need to be solved. While those extra information gain are considered as random in this study, the future study can maximize removing uncertainty by considering the standard deviation (Folsom et al., 2021) and spatiotemporal correlations (Darko et al., 2020).

Future research goals include using a region-based model with a mesoscopic fundamental diagram (Yildirimoglu et al., 2015). A mesoscopic region-based model could improve traffic state observability, improve computational efficiency on larger networks incorporating highways and freeways, and reduce uncertainty compared with microscopic link-level frameworks and macroscopic frameworks (Aghamohammadi and Laval, 2018). While this research focused on drivers, the informed driver model can also be applied to Connected Autonomous Vehicles (CAVs) in a mixed autonomy network where the centralized framework improves the efficiency with which DSO equilibrium is reached.

Additionally, by considering the spatiotemporal correlation between paths based on historical data or prior simulations, it may be possible to further improve DSO computational time. The number of calculations required to estimate the path marginal cost would be reduced in this case, since the path marginal cost can be inferred from the spatiotemporal correlation between various routes. Including spatiotemporal correlation in a region based model which includes between-region marginal costs could further improve performance by reducing the number of calculations needed to determine the marginal cost within each region and providing additional methods of parallelization such as network partitioning (Yahia et al., 2018).

While the benefit of the proposed informed decision after the first day is much less, there are still remaining memory impacting the choice, influenced by the first day. This paper targets the DSO before converging to equilibrium, but by finding the percentage of drivers that should be informed, we could lower the within-day delays and converge equilibrium sooner. By using the

output from this study, future studies could optimize the percentage of drivers to be informed to minimize within-day delays.

The informed decision making also can be applied to other system decision-making to mitigate traffic congestion. While predictive sensor location (Park and Haghani, 2015; Park et al., 2018) and emergency allocation (Park et al., 2016) problems with anticipated future depended on simulation of uninformed drivers, how information would change the driving behavior to change the system optimal decisions can provide more practical solutions.

Part 2: Temporal Multimodal Machine Learning

Methodology

The main contribution in this part is the development of a new family of online predictive decision making models, Temporal Multimodal Multivariate Learning (TMML), that can indirectly learn and transfer online information from multiple modes of probability distributions and multiple variables between different time stages, which can be applied to many routing problems under uncertainty. Preliminary remedy partially filled **this** gap by grouping similar types of locations based on their classified output, used in optimizing vehicle routing to improve the prediction uncertainty proven to be superior to partially observable Markov decision processes. Locations with broad bimodal distributions offered the greatest potential delta between the expected and true savings. We expand this bimodal learning to multimodal learning and the maximum information gain is accomplished by identifying the time-dependent similarity between the probability distribution of variables. With existing routing algorithms, opportunities for data collection are commonly skipped or missed entirely. A technology to collect more valuable observations while carefully spending system resources will add significant value to the autonomous decisions. The result will be an increased likelihood of encountering unexpected scientific discoveries, creating new opportunities to characterize uncertainties, reconciling the desire to explore further with the desire to explore in-depth, and eliminating the dichotomy between engineering limitations and discovery. Cells in the grid of Figure 17 with a similar combination of distributions are clustered together based on the similarity between the combinations (e.g., 6 cells outlined in black).

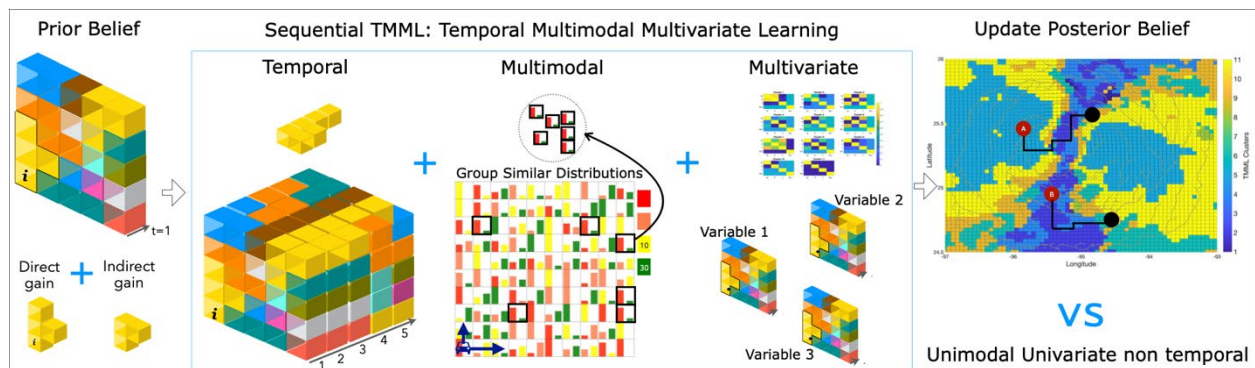


Figure 17 Online gain in temporal, multimodal, and multivariate prediction uncertainty between prior and posterior. Each cell can be assumed to have a combination of discrete travel time distributions (i.e., 2, 5, 10, 30min) with different weights.

As users traverse the map, exploration of a cell in a cluster will remove the travel time uncertainty of other cells in the same cluster. In other words, exploring one cell of the cluster will identify which of the two travel time distributions applies to that explored cell, and to all other unexplored cells in the cluster. However, each cell has two travel time distributions with peaks of different heights. Therefore, we do not update all cells that share a single travel time distribution; we update cells that have similar combinations of distributions. This technique can be applied to several real-life applications. For example, assume that each cell with heterogeneous users

presents a mixture of traffic conditions. An online RL simplifies multimodality to a unimodal distribution $X \sim N(35, 102)$ resulting in a lost opportunity to remove uncertainties in other locations. Several techniques learn and transfer information gained from multimodal distribution data in information theory for global uncertainty removal: grouping similar combinations of distributions, sampling from similar groups and updating posteriors, and solving probabilistic optimization for online routing. Those are necessary to optimize the probabilistic global routing problems based on knowledge learned and transferred in a sequence, and data is typically obtained from parts and not analyzed as a whole. While previous research addressed bimodal learning and full uncertainty removal, we address multimodal learning integrated with partial information gains from temporal and multivariate learning applied to urban traffic and hurricane data.

Multimodal Learning

Traditional machine learning frameworks overlook simultaneous observations of more than one outcome variable in different locations and times without lowering the prediction errors. Real-life data, behaviors, and problems (referring to objects, values, and attributes) are non-independent and non-identically distributed, whereas most analytical methods assume independent and identically distributed (IID) random variables. Unfortunately, the interdependent event relationship has been overlooked and future posterior events have been assumed independent from other events and systems. The dynamic impact area of a prior event could predict the probability of posterior events. However, when frequent minor events occur in a sequence, due to high uncertainty, the literature could not reliably predict the dynamic spatiotemporal evolution of a mutual relationship between events. Machine learning with rule extraction partially alleviates Black box issues, but without an effort to reduce uncertainty by observing a ground truth, the routing solutions are still unreliable and intractable. In this paper, those dependencies are partially addressed by clustering multidimensional correlation data from multiple variables through deep clustering and when one cluster is updated, other variable data from the same cluster are also updated.

Reduced uncertainty in bimodal travel time information can be processed and transferred from one agent to another agent. A prototype of bimodal uncertainty removal in an 10×10 grid map is extended to multimodality of each cell through clustering similar probability distributions for multimodal learning. The agent is allowed to move in four directions: up, down, left, and right. Diagonal moves are not allowed. Cells in the grid are numbered row-wise, starting with zero for the first cell. Grids are used because the prior state of the map will be defined using image analysis, which defines the state of a region using pixels of a fixed size. Those 2, 5, 10, and 30 minutes from bimodal is expressed as clusters. The key statistics for travel time distribution in each cell are based on lower and upper bounds, with probability $P(T)$ represented as real numbers between 0 and 1 in the model further extended to incorporate multimodality. In this project, multimodal learning enhances the value of autonomous vehicles by finding the best routes based on the desired level of exploration, risk, and constraints. In the proposed exploration framework, each grid cell contains a unique probabilistic distribution of travel time for formulating the best options to travel with partial, sequential, and mixture of information gain, with various probability distributions.

Prediction uncertainty in travel time is improved by considering Temporal Multimodal Learning (TML) on real-world traffic data. Let C be the set of all links, traffic message channels (TMCs), across the network and T be a finite set of discrete-time intervals over the morning peak period [29, 30]. We consider 39 TMCs ($|C| = 39$) on **Interstate 540 in Raleigh, NC** during 24 ten-minute time intervals from 8:00 am to 12 noon ($|T| = 24$). Probe-vehicle-based speed for each TMC was obtained from the National Performance Management Research Data Set (NPRMDS).

NPRMDS contains the travel time and speed information for each TMC for each time interval across different days over the course of eight months. Due to the day-to-day traffic randomness, the traffic speed on TMC $c \in C$ for time interval $t \in T$, denoted by v_c^t , is a random variable. As argued in the literature [19,28, 40], v_c^t is likely to have a probability distribution with multiple modes (multimodal distribution). We learn and predict v_c^t within day by analyzing the spatiotemporal correlations between random variables v_c^t for all $(c, t) \in C \times T$. By clustering all v_c^t variables, we identify spatiotemporal patterns and different combinations of traffic speed distributions with following steps:

- Analyze the spatiotemporal probability distribution of variables v_c^t by aggregating variation of traffic speed for a specific time interval across eight months. For this case study, we assume that the only factors influencing travel time are the location of TMC (c) and time-of-day interval (t).
- Clustering is performed across all C and T using minimum message length criteria to identify TMC's with similar probability distributions [38]. Clustering algorithm will automatically discover the optimal number of clusters.

Kalman Filtering (KF) Prediction v_c^t . We model the evolution of random variable v_c^t from one 10 minute interval to the next interval within-day with and without information gain using KF. The data of v_c^t acquired from TMCs have inherent noise due to sensor errors. Employing KF can produce an accurate estimate of v_c^t using noisy measurements over the period (24 intervals of time). In this paper, the traditional KF is expanded to consider the information gain from the clustering step. We model evolution of variable v_c^t from the first time interval $t = 8 - 8:10am$ to the last interval $t = 11:50 - 12pm$ within a day. Figure 4 shows the KF process which is formulated in the following equations.

Prediction step. Projection of the state at time t using the prediction at previous time $t - 1$ is given by:

where,

$$\hat{x}_t^- = A\hat{x}_{t-1}^+ + B\mu_t$$

- \hat{x}_{t-1}^+ is the state vector of the process at time $t - 1$. In this case, state vector considered is $\begin{bmatrix} \text{speed} \\ \text{acceleration} \end{bmatrix}$, where, acceleration is defined as the rate of change of speed of TMC with respect to previous time period.

- Matrix A is the state transition matrix of the process from the state at $t - 1$ to state at t and is assumed stationary over time. That is, $A = \begin{bmatrix} 1 & dt \\ 0 & 1 \end{bmatrix}$
- $dt = 1$ according to definition of acceleration defined above.
- Matrix B is a matrix of all zeros as there is no known external control input factor that affects speed measurement.

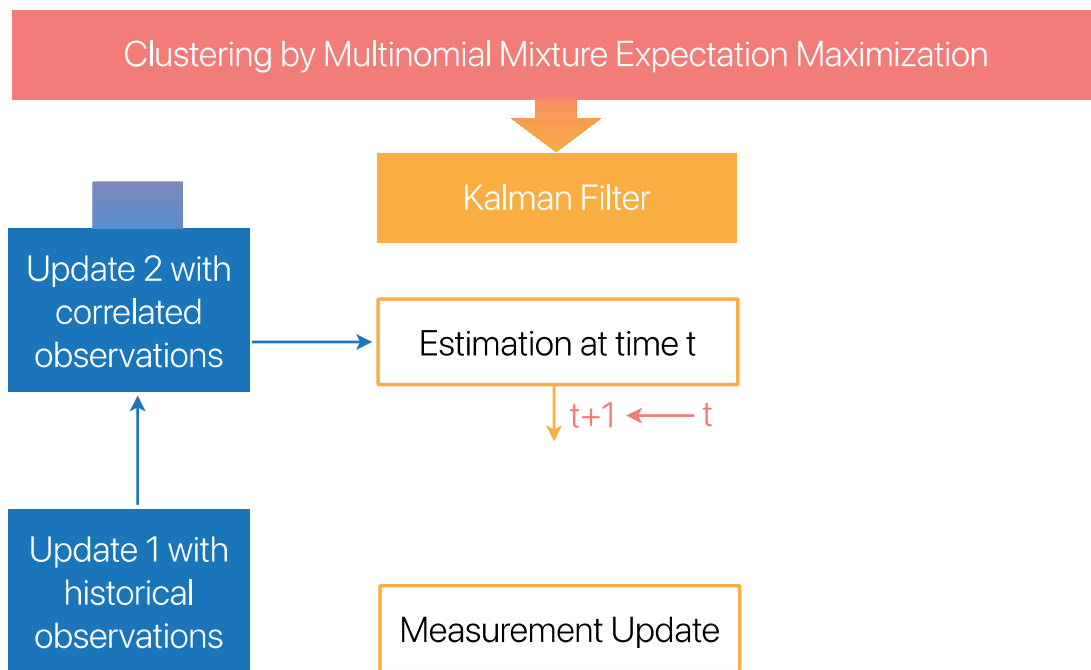


Figure 18 Two steps in KF-TML: In the predict step, a model is employed to predict the chosen state variable at next time interval $t+1$ using measurement from previous time interval (k). In the update step, the predicted state is corrected using the noisy measurements at $t+1$

- P is the error covariance matrix. It is interpreted as the error in estimation according to filter.
- Q is the process noise defined as $Q = \begin{bmatrix} 0.04 & 0 \\ 0 & 1 \end{bmatrix}$
- We assumed the speed with a variance of 0.04 in prediction step.

Projection of error covariance of state

$$P_t^- = P_{t-1}^+ A^T + Q$$

Correction step. In this step, we determine the Kalman Gain at time t (denoted by K_t) which can be interpreted as,

$$\text{Kalman gain} = \frac{\text{Uncertainty in prediction}}{\text{Uncertainty in prediction} + \text{measurements}}$$

We can write,

$$K_t = P_t^- H^T (H P_t^- H^T + R)^{-1}$$

where, H is the connection matrix between the state vector and the measurement vector and R is the data precision matrix. In our case, $H = [1 \ 0]$.

In the next step of KF, speed prediction is updated using observations Z_t . In case of KF-no TML, Z_t are the speed observations on a given day while in case of KF-TML, Z_t are mean and variance of historical speed data.

$$\hat{x}_t^+ = \hat{x}_t^- + K_t(Z_t - H\hat{x}_t^-)$$

Error covariance matrix is also updated in this step using the Kalman gain.

$$P_t^+ = (I - K_t H) P_t^-$$

KF-TML has an additional step as the speed prediction update with data Z_t^+ obtained from information gain of correlated links.

$$\hat{x}_t^{++} = \hat{x}_t^+ + K_t^+(Z_t^+ - H\hat{x}_t^+)$$

This step also updates the error covariance matrix.

$$P_t^{++} = (I - K_t^+ H) P_t^+$$

The hat operator indicates an estimate of a variable. The superscripts -, + and ++ denote predicted (prior), updated 1 (posterior 1) and updated 2 (posterior 2) estimates, respectively. The posterior 1 will be the final prediction in KF-no TML while posterior 2 will be final outcome in KF-TML.

During the update step, observations available from the correlated links from previous time intervals are considered. The mean and variance of speeds of all correlated links are used as the new observation in the update step. Therefore, traditional KF has only one update step but in this project, the algorithm is modified to have two updates, one with mean and variance of historical data of 8 months and the other with mean and variance of correlated speed data obtained from the clustering step.

The (1,1) element in matrix P denotes the variance in estimation of speed. Percentage change in $P(1,1)$ with information gain with respect to $P(1,1)$ without information gain is calculated.

$$\Delta P = \frac{P(1,1)_{\text{without info gain}} - P(1,1)_{\text{with info gain}}}{P(1,1)_{\text{without info gain}}} * 100$$

Results. The performance of KF with TML is compared against the benchmark. Traditional KF without TML ignores the correlation information where the observation is simply the observed speed from the sensor on a given day, and KF with TML is modified to include the mean observation of speed from other TMCs and previous time-periods that are within the same cluster as the given TMC and time-period. Figure 20 shows that the KF prediction with TML has fewer errors compared to the KF prediction without TML.

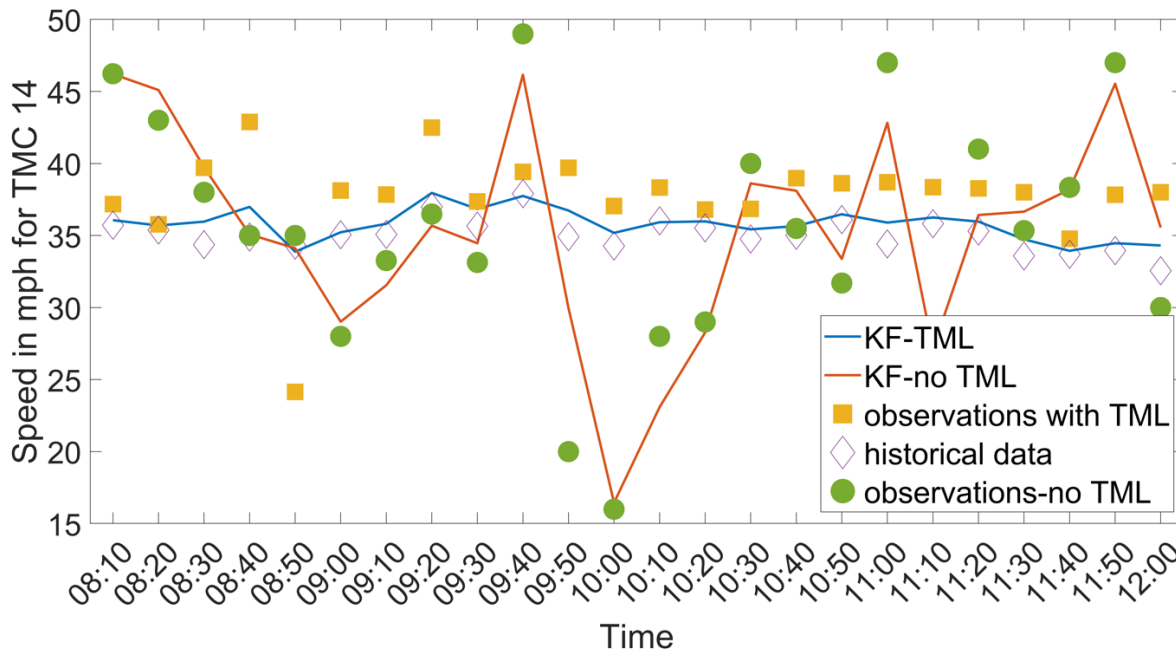


Figure 19 Speed predictions with and without TML and corresponding observations

Figure 21 shows the percentage change in uncertainty of predictions when TML is considered. A significant reduction in uncertainty indicates more confidence in the predictions with TML. In KF without TML, the update step uses measurements with noise at time t to get accurate predictions at time step t . In KF with TML, we improve the prediction performance of traditional KF by using the correlated observations from previous periods and it helps to achieve the estimation of speed at t on the previous time step, $t - 1$. This improved method is useful in getting more accurate predictions ahead of time. When speed observations with TML are close to historic observations, the reduction in uncertainty is higher.

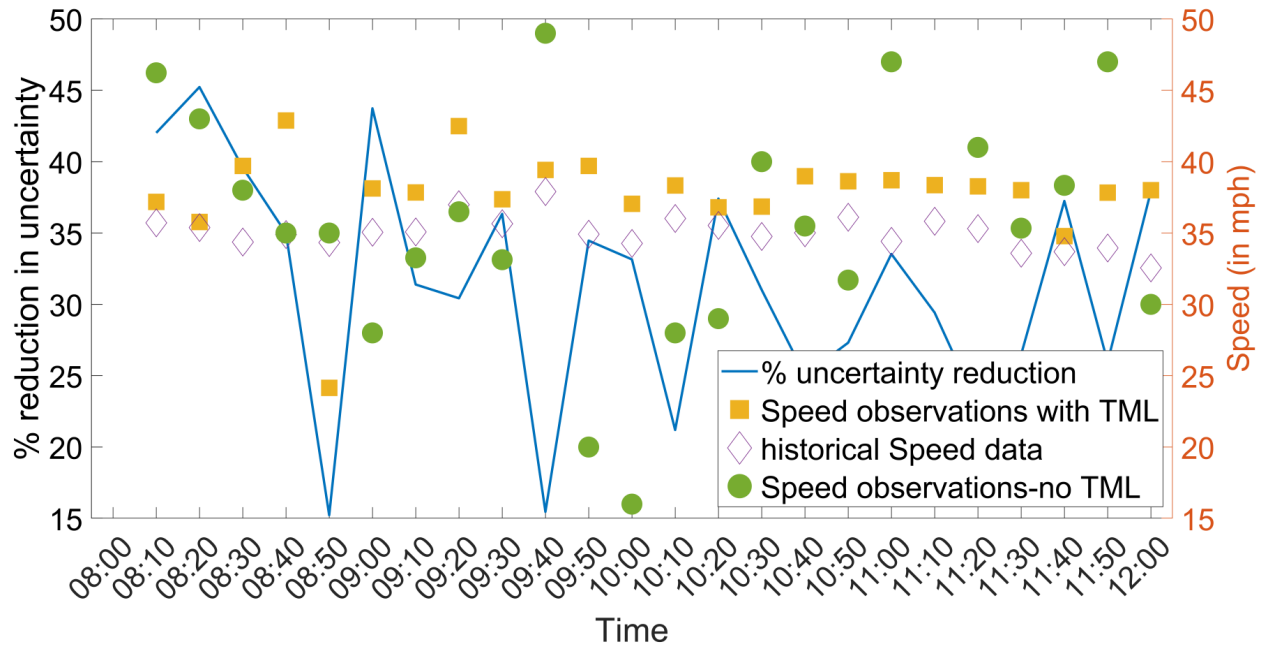


Figure 20 Percent change in uncertainty of KF prediction when TML is considered.

The Limitation and Future Study

In this project, the travel time data space is grouped into fine grain cells featuring multimodal and multivariate clusters. Rather than handling individual data points, we analyze which parent distribution those available sample observations belong and evaluate the importance of observations to be used in improving the current prediction. We overcome the limitation of traditional direct (geographically nearby) learning by the transferring online information through indirectly learning of multiple modes of probability distributions and multiple variables across different time stages.

The proposed approach will be useful for traffic and planning agencies knowing how much sample observations they need to improve the traffic prediction capability and plan the future projects. Our tool simply suggests how to use those unused values in the older forecasts, balances the older and recent forecast values based on their importance, and help improving current forecast of traffic value of interest.

References

- Aghamohammadi, R., and Laval, J. A. (2020). Dynamic Traffic Assignment Using the Macroscopic Fundamental Diagram: A Review of Vehicular and Pedestrian Flow Models. *Transp. Res. Part B Methodol.* 137, 99–118. doi:10.1016/j.trb.2018.10.017
- Amdahl, G. M. (1967). "Validity of the Single Processor Approach to Achieving Large Scale Computing Capabilities," in Proceedings of the April 18-20, 1967, Spring Joint Computer Conference (New York, NY, USA: Association for Computing Machinery, AFIPSSpring) 67. 483–485. doi:10.1145/1465482.1465560
- Angelelli, E., Morandi, V., Savelsbergh, M., and Speranza, M. G. (2021). System Optimal Routing of Traffic Flows with User Constraints Using Linear Programming. *Eur. J. Operational Res.* 293, 863–879. doi:10.1016/j.ejor.2020.12.043
- Angelelli, E., Morandi, V., and Speranza, M. G. (2018). Congestion Avoiding Heuristic Path Generation for the Proactive Route Guidance. *Comput. Operations Res.* 99, 234–248. doi:10.1016/j.cor.2018.07.009
- Avineri, E., and Prashker, J. N. (2006). The Impact of Travel Time Information on Travelers' Learning under Uncertainty. *Transportation* 33, 393–408. doi:10.1007/s11116-005-5710-y
- M. Ben-Akiva, D. McFadden, and T. et al. Gärling. 1999. Extended Framework for Modeling Choice Behavior. *Marketing Letters* 10 (1999), 187–203.
- Bureau of Public Roads (BPR) (1964). Traffic Assignment Manual. Urban Planning Division, U.S. Department of Commerce.
- Darko, J., Folsom, L., Park, H., Minamide, M., Ono, M., and Su, H. (2020). A Sampling-Based Path Planning Algorithm for Improving Observations in Tropical Cyclones. *Earth Space Sci. Open Archive* 17doi. doi:10.1002/essoar.10504807.1
- Di, X., He, X., Guo, X., and Liu, H. X. (2014). Braess Paradox under the Boundedly Rational User Equilibria. *Transp. Res. Part B Methodol.* 67, 86–108. doi:10.1016/j.trb.2014.04.005
- Di, X., and Liu, H. X. (2016). Boundedly Rational Route Choice Behavior: A Review of Models and Methodologies. *Transp. Res. Part B Methodol.* 85, 142–179. doi:10.1016/j.trb.2016.01.002
- Doan, K., and Ukkusuri, S. V. (2015). Dynamic System Optimal Model for Multi- OD Traffic Networks with an Advanced Spatial Queuing Model. *Transp. Res. Part C Emerg. Technol.* 51, 41–65. doi:10.1016/j.trc.2014.10.011
- Folsom, L., Ono, M., Otsu, K., and Park, H. (2021). Scalable Information- Theoretic Path Planning for a Rover-Helicopter Team in Uncertain Environments. *Int. J. Adv. Robotic Syst.* 18, 172988142199958. doi:10.1177/1729881421999587
- Guo, Feng, Rakha, Hesham, and Park, Sangjun. 2010. Multistate Model for Travel Time Reliability. *Transportation Research Record* 2188, 1 (2010), 46–54.

Han, K., Eve, G., and Friesz, T. L. (2019). Computing Dynamic User Equilibria on Large-Scale Networks with Software Implementation. *Netw. Spat. Econ.* 19, 869–902. doi:10.1007/s11067-018-9433-y

Han, K., Szeto, W. Y., and Friesz, T. L. (2015). Formulation, Existence, and Computation of Boundedly Rational Dynamic User Equilibrium with Fixed or Endogenous User Tolerance. *Transp. Res. Part B Methodol.* 79, 16–49. doi:10.1016/j.trb.2015.05.002

Jiang, Y.-Q., Guo, R.-Y., Tian, F.-B., and Zhou, S.-G. (2016). Macroscopic Modeling of Pedestrian Flow Based on a Second-Order Predictive Dynamic Model. *Appl. Math. Model.* 40, 9806–9820. doi:10.1016/j.apm.2016.06.041

Jotisankasa, A., and Polak, J. W. (2006). Framework for Travel Time Learning and Behavioral Adaptation in Route and Departure Time Choice. *Transp. Res. Rec.* 1985, 231–240. doi:10.3141/1985-2510.1177/0361198106198500125

Lebacque, J. P., and Khoshyaran, M. M. (2013). A Variational Formulation for Higher Order Macroscopic Traffic Flow Models of the GSOM Family. *Procedia- Soc. Behav. Sciences* 20th Int. Symposium *Transp. Traffic Theory (ISTTT 2013)* 80, 370–394. doi:10.1016/j.sbspro.2013.05.021

Lighthill, M. J., and Whitham, G. B. (1955). On Kinematic Waves II. A Theory of Traffic Flow on Long Crowded Roads. *Proc. R. Soc. Lond. A* 229, 317–345. doi:10.1098/rspa.1955.0089

Litescu, S. C., Viswanathan, V., Aydt, H., and Knoll, A. (2016b). Information Dynamics in Transportation Systems with Traffic Lights Control. *Procedia Comput. Sci.* 80, 2019–2029. International Conference on Computational Science 2016, ICCS 2016, 6-8 June 2016, San Diego, California, USA. doi:10.1016/j.procs.2016.05.522

Litescu, S. C., Viswanathan, V., Aydt, H., and Knoll, A. (2016a). The Effect of Information Uncertainty in Road Transportation Systems. *J. Comput. Sci.* 16, 170–176. doi:10.1016/j.jocs.2016.04.017

Litescu, S., Viswanathan, V., Lees, M., Knoll, A., and Aydt, H. (2015). Information Impact on Transportation Systems. *J. Comput. Sci. Sci. A. T. Gates Nat.* 9, 88–93. doi:10.1016/j.jocs.2015.04.019

Macfarlane, Jane. 2019. When Apps Rule the Road: Your Navigation App Is Making Traffic Unmanageable. *IEEE Spectrum* (2019).

Mahmassani, H. S. (2001). Dynamic Network Traffic Assignment and Simulation Methodology for Advanced System Management Applications. *Netw. Spatial Econ.* 1, 267–292. doi:10.1023/a:1012831808926

Mahmassani, H. S., and Jayakrishnan, R. (1991). System Performance and User Response under Real-Time Information in a Congested Traffic Corridor. *Transp. Res. Part A General* 25, 293–307. doi:10.1016/0191-2607(91)90145-G
 Mahmassani, H. S., and Liu, Y.-H. (1999). Dynamics of Commuting Decision Behavior under Advanced Traveler Information Systems. *Transp. Res. Part C-emerging Technol.* 7. doi:10.1016/s0968-090x(99)00014-5

- MATLAB (2019). MATLAB and Signal Processing Toolbox Release 2019b. Natick, Massachusetts: The MathWorks Inc.
- Newell, G. F. (1993a). A Simplified Theory of Kinematic Waves in Highway Traffic, Part I: General Theory. *Transp. Res. Part B Methodol.* 27, 281–287. doi:10.1016/0191-2615(93)90038-C
- Newell, G. F. (1993b). A Simplified Theory of Kinematic Waves in Highway Traffic, Part II: Queueing at Freeway Bottlenecks. *Transp. Res. Part B Methodol.* 27, 289–303. doi:10.1016/0191-2615(93)90039-D
- Newell, G. F. (1993c). A Simplified Theory of Kinematic Waves in Highway Traffic, Part III: Multi-Destination Flows. *Transp. Res. Part B Methodol.* 27, 305–313. doi:10.1016/0191-2615(93)90040-H
- Osorio, C., Flötteröd, G., and Bierlaire, M. (2011). Dynamic Network Loading: A Stochastic Differentiable Model that Derives Link State Distributions. *Transp. Res. Part B Methodol.* 45, 1410–1423. Select Papers from the 19th ISTTT. doi:10.1016/j.trb.2011.05.014
- Park, B., Zhang, Y., and Lord, D. (2010). Bayesian mixture modeling approach to account for heterogeneity in speed data. *Transportation Research Part B: Methodological* 44, 5 (2010), 662–673.
- Park, H., Haghani, A., Gao, S., Knodler, M. A., and Samuel, S. (2018). Anticipatory Dynamic Traffic Sensor Location Problems with Connected Vehicle Technologies. *Transp. Sci.* 52, 1299–1326. doi:10.1287/trsc.2018.0838
- Park, H., and Haghani, A. (2015). Optimal Number and Location of Bluetooth Sensors Considering Stochastic Travel Time Prediction. *Transp. Res. Part C Emerg. Technol.* 55, 203–216. doi:10.1016/j.trc.2015.03.023
- Park, H., Shafahi, A., and Haghani, A. (2016). A Stochastic Emergency Response Location Model Considering Secondary Incidents on Freeways. *IEEE Trans. Intell. Transp. Syst.* 17, 2528–2540. doi:10.1109/TITS.2016.2519043
- Peeta, S., and Mahmassani, H. S. (1995). System Optimal and User Equilibrium Time-dependent Traffic Assignment in Congested Networks. *Ann. Oper. Res.* 60, 81–113. doi:10.1007/BF02031941
- Qian, Z., Shen, W., and Zhang, H. M. (2012). System-optimal Dynamic Traffic Assignment with and without Queue Spillback: Its Path-Based Formulation and Solution via Approximate Path Marginal Cost. *Transp. Res. Part B Methodol.* 46, 874–893. doi:10.1016/j.trb.2012.02.008
- Qian, Z., and Zhang, H. M. (2011). Computing Individual Path Marginal Cost in Networks with Queue Spillbacks. *Transp. Res. Rec.* 2263, 9–18. doi:10.3141/2263-02
- Richards, P. I. (1956). Shock Waves on the Highway. *Operations Res.* 4, 42–51. doi:10.1287/opre.4.1.42
- Simon, H. A. (1962). Models of Man, Social and Rational: Mathematical Essays on Rational Human Behavior in a Social Setting. *J. Philosophy* 59, 177–182.

- Varia, H. R., Gundaliya, P. J., and Dhingra, S. L. (2013). Application of Genetic Algorithms for Joint Optimization of Signal Setting Parameters and Dynamic Traffic Assignment for the Real Network Data. *Res. Transp. Econ. Sustain. Transp. India* 38, 35–44. doi:10.1016/j.retrec.2012.05.014
- Wardrop, J. G. (1952). Road Paper. Some Theoretical Aspects of Road Traffic Research. *Proc. Institution Civ. Eng.* 1, 325–362. doi:10.1680/ipeds.1952.11259
- Xiong, C., Chen, X., and Zhang, L. (2015). Multidimensional Travel Decision- Making: Descriptive Behavioural Theory and Agent-Based Models. *Emerald Publ.*, 213–231. chap. 10. 213–231. doi:10.1108/978-1-78441-072-820151012
- Xiong, C., and Zhang, L. (2013a). A Descriptive Bayesian Approach to Modeling and Calibrating Drivers' En Route Diversion Behavior. *IEEE Trans. Intell. Transp. Syst.* 14, 1817–1824. doi:10.1109/TITS.2013.2270974
- Xiong, C., and Zhang, L. (2013b). Positive Model of Departure Time Choice under Road Pricing and Uncertainty. *Transp. Res. Rec.* 2345, 117–125. doi:10.3141/2345-15
- Yahia, C. N., Pandey, V., and Boyles, S. D. (2018). Network Partitioning Algorithms for Solving the Traffic Assignment Problem Using a Decomposition Approach. *Transp. Res. Rec.* 2672, 116–126. doi:10.1177/0361198118799039
- Yildirimoglu, M., and Geroliminis, N. (2014). Approximating Dynamic Equilibrium Conditions with Macroscopic Fundamental Diagrams. *Transp. Res. Part B Methodol.* 70, 186–200. doi:10.1016/j.trb.2014.09.002
- Yildirimoglu, M., Ramezani, M., and Geroliminis, N. (2015). Equilibrium Analysis and Route Guidance in Large-Scale Networks with MFD Dynamics. *Transp. Res. Procedia* 9, 185–204. Papers selected for Poster Sessions at The 21st International Symposium on Transportation and Traffic Theory Kobe, Japan, 5-7 August, 2015. doi:10.1016/j.trpro.2015.07.011
- Yu, Y., Han, K., and Ochieng, W. (2020). Day-to-day Dynamic Traffic Assignment with Imperfect Information, Bounded Rationality and Information Sharing. *Transp. Res. Part C Emerg. Technol.* 114, 59–83. doi:10.1016/j.trc.2020.02.004
- Zhang, L., Chang, G.-L., Zhu, S., Xiong, C., Du, L., and Mollanejad, M. (2013). Integrating an Agent-Based Travel Behavior Model with Large-Scale Microscopic Traffic Simulation for Corridor-Level and Subarea Transportation Operations and Planning Applications. *J. Urban Plan. Dev.* 139, 94–103. doi:10.1061/(asce)up.1943-5444.0000139
- Zhou, B., Xu, M., Meng, Q., and Huang, Z. (2017). A Day-To-Day Route Flow Evolution Process towards the Mixed Equilibria. *Transp. Res. Part C Emerg. Technol.* 82, 210–228. doi:10.1016/j.trc.2017.06.018
- Zhu, S., Levinson, D., Liu, H. X., and Harder, K. (2010). The Traffic and Behavioral Effects of the I-35w mississippi River Bridge Collapse. *Transp. Res. Part A Policy Pract.* 44, 771–784. doi:10.1016/j.tra.2010.07.001

Zhu, Z., Xiong, C., Chen, X., He, X., and Zhang, L. (2015). Agent-based Microsimulation Approach for Design and Evaluation of Flexible Work Schedules. *Transp. Res. Rec. J. Transp. Res. Board* 2537, 167–176. doi:10.3141/2537-18